Effects of symmetry, methyl groups and serendipity on intramolecular vibrational energy dispersal

William D. Tuttle, Adrian M. Gardner, Laura E. Whalley, David J. Kemp and Timothy G. Wright[a]

School of Chemistry, University of Nottingham, University Park, Nottingham NG7 2RD, UK

[a] Tim.Wright@nottingham.ac.uk

Abstract

We consider two key parameters that have been proposed to be important for vibrational energy delocalization, closely related to intramolecular vibrational redistribution (IVR), in molecules. These parameters are the symmetry of the molecule, and the presence of torsional (internal rotor) modes of a methyl group. We consider four *para*-disubstituted benzene molecules and examine their vibrational character. The molecules selected are *para*-difluorobenzene, *para*-chlorofluorobenzene, *para*-fluorotoluene, and *para*-xylene. This set of molecules allows the above parameters to be assessed in a systematic way. The probe we use is zero-electron-kinetic-energy (ZEKE) spectroscopy, which is employed in a resonant scheme, where the intermediate levels are selected vibrational levels of the S_1 excited electronic state, with wavenumbers up to 1300 cm^{-1}. We conclude that symmetry, and the presence of a methyl groups, do indeed have a profound effect on "restricted" IVR at low energies. This is underpinned by serendipitous coincidences in the energies of the levels, owing to small shifts in vibrational wavenumbers between molecules, so bringing levels into resonance. Additionally, methyl groups play an important role in opening up new routes for coupling between vibrations of different symmetry, and this is critical in the transition to "statistical" IVR at lower energies for molecules that contain them. Further, the presence of two methyl groups in the symmetrically-substituted *p*-xylene causes more widespread IVR than does the single methyl group in the asymmetrically-substituted *p*-fluorotoluene.

1. Introduction

The dispersal of energy through a molecule via its vibrations can be a valuable aid to increasing its stability following the input of localized energy, such as following photoexcitation or as the result of the formation of a chemical bond.[1,2,3] This process is often termed intramolecular vibrational redistribution (IVR).[4,5,6,7,8,9,10,11,12] If the localized energy cannot rapidly be dispersed, then the nascent chemical bond may simply break again in a biomolecular reaction, reducing the reaction efficiency; while subsequent to photoexcitation, the molecule may photodissociate if the energy remains localized. The latter process often leads to radical products that can be involved in subsequent chemistry, and in biological systems can be very harmful, leading to photodamage and cancer initiation.[13] These ideas also feed into ideas of controlling the outcomes of chemical reactions via the injection of localized energy, and has recently been discussed in relation to interactions of vibrationally-excited species with surfaces.[14] If rapid dispersal of initially localized energy occurs, then it may be that the outcomes of reactions are driven simply by the total amount of energy – i.e. the Rice-Ramsperger-Kassel-Marcus (RRKM) regime[15] – rather than the specific type and location of the energy;[16] this has impacts – for example, Polanyi's rules[17] may become inapplicable.

The design of molecules that have photophysical characteristics that enable them to disperse energy quickly is important, such as in the development of more-efficient sun protection products.[13,18,19] Much ongoing work has focused on the coupling between electronic states to provide routes for energy relaxation via conical intersections; however, within the electronic states, the delocalization of energy through the chemical bond network is also of importance.[20,21] The relevant motions for this are vibrations, and (where they exist) torsions.[21,22,23,24,25] In all cases, the critical aspect is the coupling between these modes, with anharmonicity and vibration-torsional coupling being the principal facilitators for the wavenumber range studied for the present molecules, although rotations can also be important in IVR,[6,9,10,26,27,28,29] particularly in thermal samples. [30]

Trying to uncover general mechanisms and aspects of molecular structure that are important in making energy dispersal efficient, are clearly important in being able to establish principles for molecular design.[19] As a consequence, a number of research groups have studied families of molecules, where the molecular structure is systematically changed, and its effect on vibrational energy redistribution investigated. Since many biological molecules contain a phenyl ring, which often acts as the chromophore, then work on substituted benzenes is particularly pertinent. Of importance here, are the studies comparing IVR processes in *para*-difluorobenzene (*p*DFB) and *para*-fluorotoluene (*p*FT) by Parmenter and coworkers,[28,31,32] with a related study by Zewail and coworkers.[33] Although there has been some uncertainty regarding the levels excited (see discussion in Ref. 30), the key

finding was that IVR was orders of magnitude faster in *p*FT than it was for corresponding vibrational levels in *p*DFB. Although initial work suggested that rotational levels were the cause of this "acceleration" of IVR,[28] later work focused on the role of the methyl group,[32,34] with the mode of interaction being via van der Waals interaction with C-H bonds of the phenyl rings.[35] Further work by Parmenter et al. has considered vibration-torsional levels explicitly,[36,37,38] and our recent work showed how the methyl group was facilitating coupling between vibrational levels of different symmetry.[39] Interestingly, Abel and coworkers[40] studied IVR of molecules in raised-temperature, gaseous samples and concluded that the methyl group does *not* accelerate IVR, in contrast to low-pressure, or jet-cooled gas phase studies; further comments on IVR in solution are provided in a review by the same group.[41] However, note that in these ultrafast experiments a vibrational wavepacket is excited, rather than an eigenstate (see later discussion). In addition, knowledge of how solvents affect vibrational energy eigenstates in a stepwise fashion would be highly desirable in understanding such processes in more detail. Some recent work in this area has been published by Chakraborty et al. on phenol and *p*-fluorophenol complexes.[42,43]

Only occasionally remarked on in previous work,[32] is that as well as adding a methyl group when moving between *p*DFB and *p*FT, there is also a change in symmetry between these two molecules: this can be viewed as a $D_{2h} \rightarrow C_{2v}$ change in point group symmetry, if the methyl group is considered as a point mass. An asymmetric substitution is expected to increase the likelihood of coupling, but a separation of the effects that are caused by the addition of the methyl group and those caused by a lowering of symmetry is not transparent. In addition to this, different substituents will lead to alterations in the vibrational wavenumbers, and can also lead to an increase in the number of vibrations; these could lead to changes in the density of states. These aspects were considered in Ref. 32, but concluded not to be a major factor in accelerating IVR. Of note, however, is that in Ref. 24 it was concluded that in the low-wavenumber regime, the occurrence of restricted IVR is critically dependent on these small changes in vibrational wavenumbers, since they move vibrations in and out of resonance. In addition, the efficiency of coupling of a particular mode to other states has also been noted to be of importance.[24,30,44]

The role of particular vibrations in promoting IVR has been investigated by Perry et al.,[45,46] who suggested that modes that are "close to the centre of flexibility (COF)" accelerate IVR, with an internal rotor being such a COF. This idea clearly relies on the localization of vibrational modes, and so would refer to vibrations that include motion of the bonds closest to the C-CH_3 bond in molecules with a methyl group, and indeed Davies et al.[24] have discussed this in their study of toluene, toluene-α-d_3 and *p*FT. Discussions have also been presented concerning vibrations that interact with the methyl

group by virtue of out-of-plane motion of adjacent C-H bonds;[31,35,44] these can be thought of as "wafting" the CH_3 via van der Waals interactions, which allow vibrational and torsional motion to mix. Parmenter and coworkers have commented on the out-of-plane D_{20} mode[31] and modelled such interactions in a qualitative manner,[35] and such a model has been utilized by Davies et al.[44] recently. Martens and Reinhardt[47] have considered a classical model whereby low-wavenumber vibrations interact with the methyl group; they concluded that this led to chaotic effects, which are separate from the high-wavenumber vibrations.

We also note that a number of studies have tried to address the issue of the effect of symmetry on IVR.[48,49] For example, von Benten et al.[50] studied benzene, benzene-d_1 and the three constitutional isomers of difluorobenzene. They concluded that for both sets of molecules, lowering the symmetry led to an increase in the rate of IVR. Experiments were carried out in 0.5 bar of the vapour in a cell at an elevated temperature, with the excitation being a femtosecond IR laser. It is unclear, however, what explicit modes were excited for each molecule in the wavepacket in these experiments, since the 60 fs pulse employed had a width of ~300 cm^{-1}; however, these are unlikely to have been identical.

In the present work, we select four *para*-disubstituted benzenes, in order to gain control over the variation in parameters that change between them. These molecules are: *p*DFB, *para*-chlorofluorobenzene (*p*ClFB), *p*FT and *p*-xylene (*p*Xyl). We briefly describe the symmetry changes in these species first of all – see Figure 1. Between *p*DFB and *p*ClFB the point group symmetry lowers from D_{2h} to C_{2v}, and a corresponding change occurs between *p*Xyl and *p*FT, if the methyl groups are treated as point masses. However, if the methyl groups are explicitly considered, then one can also consider the molecular symmetry group (MSG) changing from G_{72} to G_{12} between the latter two molecules. Alternatively, one can view the change between *p*DFB and *p*FT and between *p*ClFB and *p*FT as the addition of a methyl group, with the point group symmetry being maintained in the latter case, again, if the methyl group is treated as a point mass. Between *p*FT and *p*Xyl the switch of a fluorine atom to a further methyl group occurs and we move from an asymmetrically- to a symmetrically substituted molecule. One can also note that between *p*DFB and *p*Xyl two methyl groups have replaced both fluorine atoms, with the point group being maintained as D_{2h}, within the assumption of point masses for the methyl groups.

Of course, as was noted above, changing the substituents will result in corresponding vibrations changing their vibrational wavenumber, although the form of the vibration is expected to remain largely the same for most vibrations – see Ref. 51. The small changes in form that do occur, lead to relatively minor changes in vibrational wavenumbers, but this is sometimes enough to cause the movement of levels in and out of resonance (see Refs. 24, 30 and later discussion herein).

In the present work, we investigate the extent of IVR for various vibrational levels from the zero-point level up to levels < 1300 cm^{-1}. Our probe is the vibrational activity excited upon ionization, monitored by zero-electron-kinetic energy (ZEKE) spectroscopy, when using a selected vibrational level in the S_1 electronically-excited state as an intermediate resonance. In Figure 2, we show vibrationally-resolved resonance-enhanced multiphoton ionization (REMPI) spectra of the $S_1 \leftarrow S_0$ transition for the four subject molecules, where various vibrations are indicated. We compare and contrast the activity between these vibrations for the four subject molecules, and also compare to the ZEKE spectra via the vibrationless origin. We have reported REMPI and ZEKE spectra for *p*FT,[24,30,39,52,53,54] and *p*ClFB[55,56] and *p*XyI[57,58] previously, where the assignments are discussed in detail. The spectra of *p*DFB were recorded for the present work, and although two of the *p*DFB ZEKE spectra to be discussed have been reported and assigned previously by Müller-Dethlefs and coworkers,[59,60] the details are hard to discern in those published images.

2. Experimental

In previous work, cited above, we have discussed the methods employed in recording the REMPI and ZEKE spectra of *p*ClFB, *p*FT and *p*Xyl. The spectra reported herein have been recorded using the same methods and so these are only very briefly covered here.

The REMPI and ZEKE apparatus employed has been described previously in detail elsewhere.[52,61] In each case, the vapour above a room temperature sample was seeded in ~1.5 bar of Ar and the gaseous mixture passed through a General Valve pulsed nozzle (750 µm, 10 Hz, opening time of 180–210 µs) to create a free jet expansion. The excitation laser was a dye laser (Sirah Cobra-Stretch) operating with C540A or C503, depending on the molecule and energetic region of interest. The ionization laser was a dye laser (Sirah Cobra-Stretch) operating with C540A, C503 (for *p*DFB and *p*ClFB), DCM or Pyromethene 597 (for *p*Xyl and *p*FT). The two dye lasers were pumped by either a Surelite I or Surelite III Nd:YAG laser, which varied in different experiments. For the C540A and C503 laser dyes, the third harmonic (355 nm) was used to pump the dye laser, and for the DCM and Pyromethene 597 laser dyes, the second harmonic (532 nm) was used to pump the dye laser. The fundamental frequencies produced by each dye laser were frequency doubled using BBO and KDP crystals as appropriate.

The focused, frequency-doubled outputs of the two dye lasers were overlapped spatially and temporally and passed through a vacuum chamber coaxially and counterpropagating. Here, they intersected the free jet expansion between two biased electrical grids located in the extraction region of a time-of-flight mass spectrometer, which was employed in the REMPI experiments; these grids were also used in the ZEKE experiments by application of pulsed voltages, giving typical fields (*F*) of

~10 V cm^{-1}, after a delay of up to 2 μs, where this delay was minimized while avoiding the introduction of excess noise from the prompt electron signal. Bands had widths of ~5-7 cm^{-1}, even when $\sqrt{F}$ relationships would suggest the widths should be significantly greater, because of the well-known decay of the lower-lying Rydberg states accessed in the pulsed-field ionization process.[62]

3. Results and Discussion

Nomenclature and IVR

In the REMPI experiments, we are probing the $S_1 \leftarrow S_0$ electronic transition, while in the ZEKE experiments we are probing the $D_0^+ \leftarrow S_1$ transition, with D_0^+ labelling the ground electronic state of the cation. We shall employ the D_i labels of Ref. 51 for the vibrations, and generally refer to the symmetry of vibrations using the point group symmetry classes – the reader is referred to that work for the form of each of the vibrations. Since we employ free-jet expansions, the molecules will initially be almost exclusively in their zero-point vibrational energy level of the S_0 ground electronic state. Because of this, and since we shall explicitly note the S_1 intermediate level we employ for the ZEKE experiments, we shall usually omit the lower vibrational level when specifying transitions. Later, we shall need to refer to the torsional levels of *p*FT and *p*Xyl, where we use a single, m, or pair, $\{m_1, m_2\}$, of quantum numbers to label these, respectively – see Ref. 57 for more details, note that the molecules will not all be in their lowest torsional level because of nuclear spin effects – see later. In addition, when vibration-torsional (vibtor) levels arise from vibration-torsional coupling, then both the vibrational and torsional quantum numbers will be specified.

When discussing IVR, the non-interacting levels are termed zero-order states (ZOSs);[8] these ZOSs can be torsional or vibrational, while the levels that arise from interaction between these are termed vibrational (or vibtor) levels. Felker and Zewail et al.[4,5,6,7,63] have argued that there are three regimes of IVR, covering non-existent, restrictive and dissipative (or statistical), and discuss these in the context of anthracene and deuterated anthracene, noting also that these regions have been identified in other molecules, such as azulene.[64] As we shall see below, the set of molecules we have chosen exhibit each of these regimes. If two ZOSs (of whatever type) interact to form two eigenstates, then this is termed a Fermi resonance (FR), while if a small number of ZOSs interact, this can be termed a "complex Fermi resonance"; each are examples of restricted IVR. In an electronic transition, often only one of the coupled ZOSs is "bright", i.e. carries oscillator strength and as such it is only by virtue of the interactions that other ZOSs are seen – this leads to the concepts of zero-order bright (ZOB) states and zero-order dark (ZOD) states. (Note that whether a ZOS is "bright" or "dark" will depend on the type of experiment being undertaken.) If there are many ZOD states coupled to the ZOB state, then they

are termed “bath states”. There is an interesting regime when only one or two ZOD states are coupled to the ZOB state strongly, but these also couple efficiently to the bath states. This gives rise to the “tier model” (see Refs. 4 and 8), with the strongly-coupled ZOD states being termed “doorway states”.

We note that vibrational ZOSs can be thought of as “diagonally” anharmonic, but it is the result of “off-diagonal” anharmonicity that leads to interactions between ZOSs. Further, in the absence of photophysical effects, such as internal conversion and intersystem crossing, the eigenstates will have a constant population – the idea of IVR comes from time-resolved experiments where a number of eigenstates are excited coherently in a wavepacket, and the changing phases of these gives the appearance of population changes.

The impact of symmetry is clearly related to the density of states (DOS), with higher symmetries expected to lead to lower DOSs for each of their particular symmetry classes. At what energies the IVR regimes occur for a particular molecule will depend on the build-up of the DOS, and we emphasise that in the lower wavenumber regions, this is expected to be erratic (see later), but will become increasingly smooth and monotonic at higher wavenumber.

In previous work, we have discussed the phenyl-localized vibrations of *para*-disubstituted benzenes in detail[51] and noted that there is very little change in the form of these vibrations across all common substituents. As such, we have put forward a scheme, used herein, that gives these vibrations the same label across different molecules – see Table 1. However, there are a few cases where some caution is merited, particularly when switching between a symmetrically-substituted molecule and an asymmetric one, such as between *p*DFB and *p*FT. For example, in the symmetrically-substituted *p*DFB molecule, the D_5 and D_6 vibrational modes contain in-phase and out-of-phase stretches of the C-F bonds, while in an asymmetrically-substituted species such as *p*FT, the D_6 mode is largely a C-CH_3 stretch, while the D_5 mode is largely a C-F stretch, and both are of a_1 symmetry, if C_{2v} symmetry is assumed.[51] In contrast, the symmetry of the asymmetric D_6 vibration in *p*DFB is b_{1u} and so is different from that of the symmetric D_5 vibration (a_g). These differing symmetries may be expected to affect the allowed vibrational interactions and also the Franck-Condon activity in transitions. We shall comment on this further, in the below.

The interpretation of the presented spectra relies on the fact that that the ionization process is fast, and so a ZEKE spectrum generally gives a picture of the populated intermediate S_1 level(s) as mapped onto the cation eigenstates. (The effect of the laser pulse duration and power density on IVR experiments has been discussed in Ref. 30.) In cases where the intermediate level has a single ZOS contribution, then the ZEKE spectrum is expected to be well-resolved, generally with a strong $\Delta v = 0$

band, together with associated Franck-Condon (FC) active bands. The latter arise from both geometry changes between the S_1 state and the cation, but can also occur if the forms of the vibrations changes between levels (i.e. Duschinsky rotation); it is also the case that some Herzberg-Teller bands are active. If, however, the intermediate level arises from a FR between two ZOSs then, for the nanosecond laser pulses used herein, the ZEKE spectrum will appear as a juxtaposition of the expected individual ZEKE spectra of the ZOSs. Finally, if the intermediate level is a mixture of numerous ZOSs, then the ZEKE spectrum will be a juxtaposition of all contributions from these and this would result in a ZEKE spectrum where little structure was resolvable. Time-resolved photoelectron studies[4,5,6,7,8,9,10,11,12] are useful for unpicking the details of the coupling (although caution is required in their interpretation[10]); in particular, since the t = 0 spectrum can be obtained, which will usually be a good representation of the ZOB state. Subsequently, the evolution of the spectrum can be followed as a function of time to unpick the various interactions occurring. In principle, frequency-resolved spectra (such as here) will allow the same detail to be recovered,[8,39] but this is only feasible when clear structure is still seen in the spectrum.

Initial comments

In Figure 2, we show the 0–1400 cm^{-1} regions of the REMPI spectra of the four molecules under consideration. We have given assignments of the main bands based upon previous work (see above), noting that the low wavenumber regions of the spectra of *p*FT and *p*Xyl contain many weak bands arising from torsional and vibtor levels.

In Figures 3–5 we show a series of ZEKE spectra for the four molecules, *p*DFB, *p*ClFB, *p*FT and *p*Xyl; in each case, exciting through the same intermediate level: S_1 0^0, $S_1 9^1$ and $S_1 5^1$, in order of increasing energy. (Note that we show the form of the relevant vibration in Figures 4 and 5.) As we can see from Figure 3, all four of the ZEKE spectra obtained when exciting via $S_1 0^0$ have well-defined bands, with a flat baseline between all of the features. We note that several totally-symmetric vibrations are active across the spectra, allowing their wavenumbers to be established (see Table 1), for *p*Xyl a number of these will be noted again later on, in relation to other spectra, but we note here the 3^1 transition is present, but within a small group of bands, and so only an approximate value is obtained for D_3 in the cation of ~1634 cm^{-1}. In Figure 4, we can see that there is essentially a flat baseline across the spectra for *p*DFB and *p*ClFB, while in *p*FT and *p*Xyl there are indications of some congestion coming into the spectrum, and this is a little more pronounced for *p*Xyl than *p*FT. Finally, in Figure 5, we see again, essentially flat baselines, with well-defined bands for *p*DFB and *p*ClFB, but there is a significant amount of congestion in the *p*FT spectrum, and this is extremely pronounced in the case of *p*Xyl.

Our interpretation of the series of ZEKE spectra in Figures 3–5 is that vibrational interactions are minimal at low wavenumbers in *p*DFB and *p*ClFB, being localized to a few Fermi resonances, but clearly significant interactions occur in *p*FT and to a greater extent in *p*Xyl, as judged by the appearance of the spectra in Figs. 4 and 5. On this basis, we can conclude that the change in point group symmetry is having a limited effect, since *p*DFB belongs to D_{2h} and *p*ClFB belongs to C_{2v}. This is perhaps somewhat surprising, as there are almost twice as many totally-symmetric (a_1) vibrational normal modes for *p*ClFB than there are for *p*DFB (a_g). One stark manifestation of this difference is the strong 6^1 transition in *p*ClFB that is absent in *p*DFB (since the D_6 vibration is of b_{1u} symmetry in the latter molecule). Since, interactions will occur between fundamentals, overtones and combination levels then it is the build-up of the latter two type of levels that is expected to drive the extent of vibrational coupling.

If we regard the CH_3 group as a point mass, then both *p*FT and *p*ClFB belong to the C_{2v} point group, and *p*ClFB has many of its vibrations at a lower wavenumber than those in *p*FT, yet *p*FT shows much more extensive IVR than does *p*ClFB. (While it is true there are eight extra vibrations in *p*FT from the methyl group, as well as the torsion, there is not expected to be any significant effect from these, largely since most of these are of a high wavenumber.[32]) In a similar vein, *p*DFB and *p*Xyl each have D_{2h} point group symmetry, again if we regard the CH_3 groups as point masses, and these will have similar vibrational wavenumbers as the masses of F and CH_3 are similar.[51] Again, there are additional vibrational modes (sixteen extra) from the methyl groups, but again, by analogy with *p*FT, these are not expected to have a significant effect in this wavenumber range. Despite this, it is clear that the interactions in the symmetrically-substituted *p*Xyl molecule are significantly greater than that in the symmetrically-substituted *p*DFB; further, these are greater than the asymmetrically-substituted *p*FT and *p*ClFB molecules. Clearly, other factors than simply vibrational interactions need to be considered, and the main factor will be shown to be vibrational-torsional coupling.

Vibration-torsional coupling

The possible role of vibration-torsional coupling in promoting IVR was put forward by Parmenter and coworkers some time ago,[31] but this was more by implication after concluding that other factors were unlikely to be playing a key role in the increased IVR in *p*FT compared to *p*DFB.[32] More explicit evidence that vibration-torsional coupling is prevalent in substituted benzenes containing a methyl group was put forward by Lawrance and coworkers in their detailed studies on toluene using two-dimensional laser-induced fluorescence (2D-LIF),[22,25] and these ideas have also been employed in the interpretation of time-resolved photoelectron studies of IVR[23,24] and in our ZEKE[24,30,39,52,53,54] and 2D-LIF[39] studies. Of particular note is that in the work of Lawrance and ourselves on toluene and *p*FT, vibtor levels have been assigned that may be viewed as combination bands of vibrational and torsional states, which are

symmetry-allowed under the G_{12} MSG, and these can be treated as ZOSs. Further, ZOSs of the same MSG symmetry class can interact, in an analogous manner as FR for pure vibrational levels. These interactions lead to mixings between the levels, causing bands to have unexpected intensities, and also be in shifted positions. In a *tour de force*, a comprehensive deperturbation analysis was achieved for toluene[22] and the same ideas have been applied to *p*FT.[65]

In very recent work,[39] we provided direct evidence for coupling between vibrations of different symmetry in *p*FT, which was facilitated by vibration-torsional mixing. Owing to the lowest nuclear spin states having different symmetry, it is not possible to cool the population of the m = 1 torsional level into the m = 0 level via collisions, and both survive in the jet expansion and so may be termed "cold" torsional levels (where m is the torsional quantum number).[22,57] This means transitions can occur out of either of these torsional levels, and we noted in Ref. 39 that this opens up the possibility of observing interactions that involve both a_1 and a_2 vibrations for the m = 1 level, and similarly for b_1 and b_2 vibrations; further, Herzberg-Teller (HT) coupling then opens up the possibility for all C_{2v} classes of vibration to interact. By considering all vibrational and vibtor levels in the relevant wavenumber region, we were able to show that there were many more routes for the $2D_{18}$ m = 1 vibtor level to interact with other ZOSs, than the (torsionless) $2D_{18}$ m = 0 level. Thus, this showed direct evidence for how the methyl group was facilitating interactions between vibrations in this molecule; particularly noting coupling of b_1 symmetry combination vibrations (ZOD states) with an a_1 symmetry overtone (the ZOB state). Further, it was clear from the analysis that there were very few totally symmetric pure vibrational levels that could interact with the D_{18} overtone, and it was the role of the methyl group in both the relaxation of the symmetry criteria for coupling vibrations and the increase in the DOS that caused the dramatic increase in coupling.[39]

The results shown in Figures 3–5 clearly show that the effect of point group symmetry lowering on moving from *p*DFB to *p*ClFB is small and confirm that the dramatic rise in IVR between *p*DFB and *p*FT is not a point group symmetry effect, nor a result of small changes in ring-localized vibrations, but a direct effect of the presence of the methyl group.

We now extend these arguments to the comparison of *p*DFB, *p*FT and *p*Xyl. Since the point group symmetry of both molecules is the same (considering CH_3 as a point mass) and the masses of CH_3 and F are quite similar, then one might have expected the extent of vibrational coupling in both species also to be similar. Notably, it is initially surprising that coupling in *p*Xyl is significantly more pronounced than in *p*FT, since the higher (effective) point group symmetry of the former might be expected to lead to reduced vibrational coupling, as there would be fewer a_g modes in the former than a_1 modes in the

latter. That this coupling scenario is far from the case may be rationalized by invoking vibration-torsional coupling.

In Ref. 57, we discussed the torsional levels of *p*Xyl in detail, in terms of the G_{72} MSG. For this molecule, we label each torsional level with two quantum numbers, one for each CH_3 group; levels can thus be designated {m_1, m_2}, with {0,0} being the lowest, torsionless level; additionally, there may be superscripts to indicate particular combinations of levels.[57] We also showed that the lowest four torsional levels, {0,0}, {0,1}, {1,1} and {1,-1} had different nuclear spin symmetries and hence all should remain populated in the jet expansion, and hence may be termed "cold" torsional levels. In principle, therefore, excitations can occur from any of these, and we labelled the REMPI spectrum in Ref. 57 indicating this. (For clarity, in the REMPI spectrum in Figure 2, here, we have omitted much of the details of the torsional levels.)

In Table 2, we show the MSG symmetries of the vibtor levels that result when the symmetry of each of the abovementioned four torsional levels is combined with the symmetries of the different vibrations. We note that a_g vibrational modes can only interact with each other in a pure vibrational picture; however, once we include vibration-torsional coupling, then the possibilities for interaction increase markedly. For example, vibtor levels formed from a_g vibrations with the {0,1} torsional level are able to combine with vibtor levels formed from the same torsional level, but with vibrations of b_{1g}, a_u and b_{1u} symmetries– all being of g'' symmetry in G_{72}. In fact, this means that the set of vibrations that can couple in *p*Xyl is the same as that in *p*FT; additionally, further pairwise couplings are possible via the {1,1} and {1,-1} torsions. Taken together, we can see that the vibtor levels of an a_g vibration can facilitate interactions with vibtor levels involving other vibrations of b_{1g}, a_u and b_{1u} symmetry in a number of ways. Further, we know HT interactions occur, which allow b_{3g} vibrations to be active in the $S_1 \leftarrow S_0$ spectrum for D_{2h} molecules such as *p*DFB and *p*Xyl, and these can similarly couple via various vibtor levels, similar to that discussed in Ref. 39 for *p*FT. If vibration-torsion coupling occurs between FC- and HT-active modes, then in fact vibrations of any symmetry class can interact via at least one of these mechanisms. A further observation is that there are more than twice as many torsional levels in *p*Xyl as in *p*FT, and concomitantly more vibtor levels for each vibrational level; as a consequence, these provide a commensurate increase in the number of interaction possibilities. It is thus clear why, despite the apparently more restrictive coupling of pure vibrations in *p*Xyl over *p*FT, in fact there are more than double the possibilities for coupling involving the vibtor levels.

Detailed comments on assignments

We now move onto a discussion of the specific interactions that are occurring in the different molecules. First, we need to discuss the assignments of the ZEKE spectra presented here for *p*DFB and *p*Xyl.

Assignment of pDFB spectra

In Figure 6, we present six ZEKE spectra of *p*DFB when exciting through six different vibrational levels of the S_1 electronic state (see Figure 2 for the REMPI spectrum). ZEKE spectra via the 0^0 and 5^1 levels have been presented before in Refs. 59 and 60 by Müller-Dethlefs and coworkers, but the others are presented here for the first time. We also note that Sekreta et al.[66] studied *p*DFB by REMPI-PES, with the 0^0, 9^1, 18^2 and 5^1 being amongst those considered. We essentially concur with the assignments of the previous REMPI-PES and ZEKE spectra, [59,60,66] but note that we have labelled the spectra with the D_i labels used herein. (Our assignments of the vibrations of the cation are also generally consistent with those of Kwon et al.,[67] who recorded one-photon mass-analyzed threshold ionization (MATI) spectra of *p*DFB.) The assignments of the spectra in Figure 6 are also consistent with the calculated wavenumbers of the cation of *p*DFB,[58] and with the expected activity, based on the assignments of the S_1 state intermediate levels recorded in fluorescence by Coveleskie and Parmenter,[68] and Knight and Kable[69] – with the assignments in the latter study being confirmed by dispersed fluorescence. We now briefly summarize the pertinent assignments of the ZEKE spectra in Figure 6.

As noted, the ZEKE spectrum via S_1 0^0 has been presented and assigned previously.[59,60] We simply note here the expected dominance of the $\Delta v = 0$ band, and the expected preponderance of activity from totally symmetric vibrations (fundamentals, overtones and combinations). Also of note is the clear presence of low-wavenumber bands of b_{2g}, b_{3u} and a_u symmetry, which are thought to arise from HT interactions in the cation.

We now move onto the ZEKE spectrum recorded via S_1 9^1, which is presented here for the first time. It shows a strong band at 437 cm^{-1}, which is straightforwardly assigned as 11^1, and so immediately it is clear that the $\Delta v = 0$ propensity rule is not adhered to. The triplet of bands to higher wavenumber at 834 cm^{-1}, 857 cm^{-1} and 877 cm^{-1} may be straightforwardly assigned to 9^1, 29^2 and 11^1. A question immediately arises as to whether the corresponding vibrations are interacting, and if so, in the S_1 state or the cation. We note that Coveleskie and Parmenter,[68] and Knight and Kable[69] suggested that the 9^1 and 11^2 levels were in Fermi resonance, with the possibility that the 29^2 level was overlapped with the combination level, $17^1 19^1$. To gain further insight into these possibilities, we show the three ZEKE spectra in Figure 6 recorded via the S_1 D_9, $2D_{29}$ and $2D_{11}$ intermediate vibrational levels (see the REMPI

spectrum in Figure 2). It may be seen that the spectrum via 29^2 shows a strong $\Delta v = 0$ band, a weak 9^1 feature, and only an inkling of the 11^2 band. The spectrum via 11^2 shows non-$\Delta v = 0$ behaviour, similar to that seen in the ZEKE spectrum of *p*FT when exciting via this level;[52,54] notably, both the 9^1 and 29^2 bands are quite weak. The absence of the 29^2 in the origin ZEKE spectrum, but its reasonable intensity in the ZEKE spectrum via D_9, suggests that the D_9 and $2D_{29}$ levels may be coupled in the S_1 state, although only weakly. However, some caution is merited in drawing conclusions from the $S_1 9^1$ ZEKE spectrum as the amount of UV is not constant across the range, and there is a drop-off in UV intensity towards the end of the presented spectra; hence, the 9^2 band would be expected to have more intensity than it appears to have. This suggests that a progression is formed in the D_9 vibration, with a similar observation having been made in *p*FT.[54] Overall, we interpret these spectra as showing a weak interaction between the D_9 and $2D_{29}$ vibrational levels in the S_1 state, and similarly between the D_9 and $2D_{11}$ in the S_1 state. We note that the observation of the strong 11^1 ZEKE band when exciting via $S_1 9^1$ corresponds to similar such activity seen in the REMPI-PES study[66] and in dispersed fluorescence,[69] and could suggest that the atomic motions of the D_{11} and D_9 modes undergo Duschinsky mixing between these electronic states. In addition, we note that when exciting via $S_1 29^2$, a new band is seen at 1032 cm^{-1}, and if this were the $17^1 19^1$ band, then it would imply a value for D_{17} in the cation of 729 cm^{-1}, which is in fair agreement with the calculated value, and so we accept this assignment. Since there does not appear to be a "partner" REMPI band, it seems that the 29^2 and $17^1 19^1$ REMPI (and LIF) bands are simply overlapping, as suggested in Ref. 69, rather than there being an interaction between the corresponding vibrational levels. Other bands in the spectra are generally straightforward to assign, and are not the focus of the present paper.

We now move onto the ZEKE spectrum recorded via the $S_1 18^2$ intermediate level. This clearly shows a strong $\Delta v = 0$ band, consistent with the REMPI-PES spectrum of Ref. 66. The assignment is consistent with a value for D_{18} in the cation of 512 cm^{-1} – a value that is in line with the reported value of ~510 cm^{-1} in Ref. 66. The rest of the spectrum consists of bands arising from totally-symmetric vibrations.

Finally, the ZEKE spectrum recorded via $S_1 5^1$ is similar to that reported in Ref. 60 and closely resembles the REMPI-PES spectrum of Ref. 66, with a strong $\Delta v = 0$ band. Our assignments concur with those studies.

Assignment of pXyl spectra

In Figure 7, we show a series of ZEKE spectra recorded for *p*Xyl with intermediate levels in the range 770–810 cm^{-1}, with the excitation positions shown in the portion of the REMPI spectrum in the inset. In addition, in the top trace we also show the spectrum recorded via the $S_1\ 0^0$ level, which extends to

higher wavenumber than the corresponding spectrum we reported earlier in Refs. 57 and 58, which focused on assignments of the S_1 levels below 600 cm^{-1}, which consist of torsions, low-wavenumber vibrations, and vibration-torsional (vibtor) levels.[57,58] We assign the spectra in Figure 7 by making reference to our previous work, but also to the calculated vibrational wavenumbers for the cation and S_1 state in Table 1 (see also Ref. 58).

We commence with the ZEKE spectrum recorded at S_1 0^0+775 cm^{-1}, which has bands at 805 and 950 cm^{-1}. The former, slightly more intense band, is straightforwardly assigned as 9^1, with the latter as 18^2. The spectrum recorded at S_1 0^0 + 803 cm^{-1} looks somewhat similar, with the same two bands present, but with the 950 cm^{-1} band the more intense. For these two spectra, we infer that the D_9 and $2D_{18}$ levels are in Fermi resonance, with the S_1 level at 775 cm^{-1} being dominated by D_9 (with the transition represented $9^1 \ldots 18^2$), while the one at 803 cm^{-1} is dominated by $2D_{18}$ (and the transition represented $18^2 \ldots 9^1$). Bands to higher wavenumber in these spectra are largely associated with combinations bands of the main $\Delta v = 0$ structure. However, it is clear that there is other structure between these bands, which is becoming broad in nature; particularly noticeable when exciting at $S_1 0^0$ + 803 and $S_1 0^0$ + 808 cm^{-1}. When exciting at $S_1 0^0$ + 808 cm^{-1}, again the spectrum is very different and the underlying broad, structure is becoming dominant. We see two clear bands at 884 and 950 cm^{-1}, with the former being assigned as 11^2 and the latter being 18^2. We can see that the 11^2 band also appears when exciting at $S_1 0^0$ + 803 cm^{-1}, but is at most extremely weak at $S_1 0^0$ +775 cm^{-1}. These three spectra suggest that: the $2D_{11}$ and $2D_{18}$ levels are interacting significantly (a Darling-Dennison resonance[70]); the D_9 and $2D_{18}$ levels are interacting strongly; but the D_9 and $2D_{11}$ levels are interacting at most weakly.

We also note the appearance of a band at 990 cm^{-1} when exciting at $S_1 0^0$ + 808 cm^{-1}. A possible assignment for this band is to $16^1 19^1$, which would suggest a value for D_{16} in the cation of 759 cm^{-1} and in the S_1 state of 595 cm^{-1}, assuming the corresponding level is resonant in S_1. These are in line with the calculated values, but we consider these assignments as tentative. To higher wavenumber, we see bands that correspond to the same ones in the $\Delta v = 0$ region, but in combination with D_{11}.

We gain insight into the activity that is underlying the main features in the $\Delta v = 0$ region by examining the low-wavenumber section of the spectrum. We have noted an aspect of ZEKE spectra in several of our previous studies, whereby we see structure to lower wavenumber that arises from "components" of combination levels, and hence gives information on the make-up of combinations that are active in the $D_0^+ \leftarrow S_1$ transition. In cases where significant mixing between levels has occurred, loss of resolved structure in the $\Delta v = 0$ region occurs, caused by the overlap of many contributions; however, we still see well-structured "component" bands to lower wavenumber, since different intermediate eigenstates arising from the same ZOSs will give activity in the same components, which then sum

up.[39] Hence, when we examine the 420–530 cm^{-1} region of the ZEKE spectra recorded at $S_1 0^0$ + 803 cm^{-1}, we see bands at 428 cm, 441 cm^{-1}, 472 cm^{-1}, 490 cm^{-1} and 518 cm^{-1}, which can be assigned as 29^1m={0,3(+)}$^+$, 11^1, 19^2 (with a possible contribution from 18^1), 11^1m={0,3(+)}$^-$ and 18^1m = {0,3(-)}$^-$; in addition, we see a weak band at 44 cm^{-1}, which is assigned as m = {0, 3(-)}$^-$ – see Ref. 57. To higher wavenumber, a very weak feature attributable to the 14^2 transition can be seen at 680 cm^{-1}. A number of these bands are reminiscent of ZEKE bands seen in our earlier work,[58] occurring in a complicated REMPI feature in the range 420–445 cm^{-1}, dominated by three bands. We note that transitions involving those three levels in combination with the D_{29} vibration would fall in the wavenumber region of the 9^1 and 18^2 bands in the S_1 state. The low-wavenumber activity thus suggests multiple contributions to the S_1 770–810 cm^{-1} region and suggests that vibronic coupling is significant, since the combinations of the totally-symmetric levels referred to above with D_{29} would be of b_{3g} symmetry in D_{2h} (a_4″ symmetry in G_{72}), and so these could interact with D_9 and $2D_{18}$ via HT coupling between vibtor levels.

When we examine the 420–530 cm^{-1} region of the ZEKE spectra recorded at $S_1 0^0$ + 808 cm^{-1}, we see one discernible band at 440 cm^{-1}, which is a Δv = -1 contribution arising from the 11^2 character. It is interesting to note that when exciting at $S_1 0^0$+775 cm^{-1} we see weaker bands at 440 cm^{-1}, 472 cm^{-1}, 486 cm^{-1}, 518 cm^{-1} and 680 cm^{-1}, with the 440 cm^{-1} and 472 cm^{-1} bands being the most prominent. The activity of these two bands, assigned to 11^1 and 18^1, are consistent with the assignments of the Δv = 0 region when exciting across the S_1 770–810 cm^{-1} range. In all spectra, the weaker features to higher wavenumber are combinations involving D_{11} and the main Δv = 0 bands: $9^1 11^1$, 11^3 and $11^1 18^2$.

Two ZEKE features appear at ~850 cm^{-1} and 870 cm^{-1} when exciting via S_1+808 cm^{-1}. The latter is consistent with a contribution from $17^1 19^1$; it seems unlikely that this arises from a coincident resonance in the S_1 state, since this would imply a value for D_{17} in the S_1 state of 595 cm^{-1}, which seems too far from the calculated value, and so we assume that the appearance of the ZEKE band is from FC activity. The assignment of a contribution from $18^1 29^1$ to the 850 cm^{-1} band is consistent with both S_1 and D_0^+ wavenumbers, which would be of a_u symmetry, but can become active via vibration-torsional coupling. This assignment also seems to fit the corresponding distinct feature in the otherwise unstructured ZEKE spectrum recorded when exciting at S_1 0^0 + 771 cm^{-1}.

We now move onto the ZEKE spectra of *p*Xyl presented in Figure 8, recorded when exciting in the range 1140–1221 cm^{-1}, with the excitation positions shown in the portion of the REMPI spectrum in the inset. It can immediately be seen that there is limited resolved structure in these ZEKE spectra. We first consider the spectrum recorded at S_1 0^0+1186 cm^{-1}. This exhibits two features: a single band at 1189 cm^{-1} and a double band with maxima at 1237 and 1249 cm^{-1}. These also appear in the ZEKE

spectrum via the origin, and can be assigned as 7^1, 5^1 and $9^1 11^1$, respectively. The wavenumber of the intermediate level, and symmetry, suggests the main REMPI band at 1186 cm^{-1} arises from 5^1, with the activity from $9^1 11^1$ either being FC in origin, or perhaps arises from FR in the cation; the 7^1 activity appears to be FC in nature. Based on the S_1 fundamentals, the $9^1 11^1$ band would be expected at 1179 cm^{-1}, and so this could also be present in the S_1 state, perhaps at position G (0^0+1177 cm^{-1}), and in FR with the D_5 level in the S_1 state.

Interestingly, when exciting at S_1 0^0+1144 cm^{-1}, we see two clear ZEKE bands on an essentially flat baseline. The wavenumbers of 1183 cm^{-1} and 1326 cm^{-1} initially suggest assignments to 7^1 and 11^3, respectively, but the intensity of the latter band is not in line with FC activity and the S_1 11^3 level is expected at 1212 cm^{-1} and so is not a viable intermediate level. In addition, the 7^1 transition does not appear to be active to any significant extent in REMPI spectra of the other molecules (see Figure 2 and related references). A possibility of $12^1 14^1$ was considered, but again the S_1 level is expected to be far from resonant at this wavenumber, and its intensity would be surprising for FC activity. Further consideration then led to the realization that the FR $9^1 \ldots 18^2/18^2 \ldots 9^1$ REMPI bands, each in combination with D_{29}, would appear at 1144 cm^{-1} and 1178 cm^{-1}, respectively; additionally, the corresponding ZEKE bands should appear at 1183 cm^{-1} and 1328 cm^{-1} and so are highly consistent with the two observed bands, and so we accept this assignment to a pair of FR bands from these combinations. What is remarkable is the difference in appearance of the two ZEKE spectra when exciting via the $9^1 29^1$ and $18^2 29^1$ FR bands, with one being a flat baseline with distinct bands, while in the other apparently all structure is essentially lost. This suggests the latter spectrum arises from an overlap of the $18^2 29^1$ FR band with another contribution: note that we mentioned above that the $9^1 11^1$ band is expected here, and so it seems that $D_9 D_{11}$ is coupled to D_5, with the loss in structure being attributable to further coupling to other levels, which then masks the ZEKE bands arising from the $18^2 29^1$ FR band.

Finally, we note that a possible assignment for the REMPI band at 1192 cm^{-1} that gives rise to an unstructured ZEKE spectrum would be to $6^1 m$={0,1}. If correct, it does not seem likely that this arises from direct interaction with the $D_5 m$={0,1} vibtor levels, as this involves two fundamentals; hence, we suggest this involves a two-step (or higher) interaction. The REMPI band at 1221 cm^{-1} that gives rise to a ZEKE band at 1578 cm^{-1} appears to be consistent with an assignment to 13^2 or 16^2. This would giving S_1 and D_0^+ values for the fundamental of 611 cm^{-1} and 789 cm^{-1}, respectively. Since we have established values for D_{16} in the S_1 and D_0^+ states of 595 cm^{-1} and 759 cm^{-1}, respectively (see above), we opt for the assignment of the 1221 cm^{-1} REMPI and 1578 cm^{-1} ZEKE bands to 13^2.

Further comments on DOS, symmetry and IVR

It is clear that when vibrational excitation at very high wavenumber is present in a molecule, coupling will be widespread amongst many ZOSs (statistical IVR). However, this is not true at very low wavenumber, where it is likely that interactions will only involve small numbers of vibrations (restrictive IVR). As we move up in wavenumber, the DOS will increase, but initially in an erratic matter, leading to clumps of levels. This clumpiness will be even more stark in electronic spectroscopy, since the levels observed in a spectrum by virtue of coupling will only be those localized around a ZOB state; alternatively, it is only when a ZOB state is coincident with a clump of levels that such coupling can be observed; further, it is clearly only the levels that actually couple to the ZOB state that will be seen. Ourselves, in collaboration with the Reid group,[24,30] have alluded to this aspect of IVR, and we have noted this again recently.[39]

In the spectra shown in the present work, this localized activity is evident. For example, considering the D_6 and the D_5 vibrations. We first note that the D_6 vibration is not active in *p*DFB or *p*Xyl, since it is not totally-symmetric under D_{2h} symmetry, but the D_5 vibration is active in all four molecules. This is a good example of how the lowering of symmetry might be expected to increase coupling. When comparing the ZEKE spectra for *p*FT via each of these two vibrations, the loss of structure due to IVR is significantly more marked for 5^1 than 6^1, even though these two vibrations are only ~36 cm^{-1} apart; this has been remarked on previously.[30] Another example would be the set of ZEKE spectra for *p*Xyl in Figure 7, where the spectrum at +771 cm^{-1} is unstructured, that at +775 cm^{-1} is well structured, and then we see broad structure building up as we move through the +803 cm^{-1} and +808 cm^{-1} spectra. The DOS will not be increasing monotonically, nor especially rapidly, across this narrow wavenumber range, and the observed behaviour seems more likely to be associated with ZOB states hitting clumps of ZOSs at particular wavenumbers and then coupling to them. We see similar variation in structuredness as we cross the series of spectra in Figure 8, with the spectrum obtained when exciting at S_1+1144 cm^{-1} being notably simple and structured.

We now look at the DOS for the four molecules in more detail. To do this, we select a ±20 cm^{-1} window around the respective D_9 and D_5 vibrations, and summarize in Table 3 the number of levels that we find, which can act as ZOSs. We first consider totally-symmetric vibrational levels only (a_1 or a_g), which would be able to couple directly to the D_9 level; we see that *p*ClFB and *p*DFB have 6 and 5 levels, respectively, and *p*FT has 6; rather surprisingly *p*Xyl has only 1, highlighting the role of serendipity in the proximity of vibrational ZOSs at these low wavenumbers. On the other hand, when we consider all vibrational levels, the respective numbers are 30, 19, 14 and 18 for *p*ClFB, *p*DFB, *p*FT and *p*Xyl respectively. We emphasise that these numbers are comparatively small, and so significant changes

can result from just a handful of levels falling inside or outside of the selected window, which itself is dependent on the wavenumber of the D_9 vibration for a particular molecule. When we look at the higher-wavenumber D_5 vibration, we see the numbers of totally-symmetric vibrational levels are, respectively, 18, 7, 21 and 9, while the total number of vibrational levels are 85, 74, 91 and 72. Thus, overall, the numbers are larger for the higher-wavenumber D_5 vibration than for the lower D_9, as expected, but not high enough to explain the dramatic changes in the appearances of the spectra. In addition, the numbers for *p*Xyl would not be expected to lead to the notable loss of structure observed compared to the other species.

We now include the effect of vibration-torsional coupling for *p*FT and *p*Xyl. Table 3 also shows the total number of totally-symmetric levels arising from either vibrational or vibtor levels. These can be seen to be 6, 5, 17 and 14 for the D_9 vibration of for *p*ClFB, *p*DFB, *p*FT and *p*Xyl, respectively. If we then include vibrational or vibtor levels that have allowed transitions from the "cold" torsional levels, the numbers become 6, 5, 47, and 169; while if we further allow HT coupling and other mechanisms that allow all of these levels to be considered as coupling to some extent, then the respective final numbers are 30, 19, 123, and 595. Thus, it becomes clear that the torsional levels do indeed lead to a dramatic increase in the DOS, and this becomes more marked as more coupling mechanisms open up. We now move to the D_5 level, where we find 18, 7, 76, and 81 totally symmetric vibrational or vibtor levels; 18, 7, 221 and 734 levels that have allowed transitions from the "cold" torsional levels; and finally overall totals of 85, 74, 610 and 2602 levels that could couple if HT coupling or other mechanisms operate. Note that we have included all phenyl-ring-localized vibrational levels up to four quanta in our analyses, and all vibtor levels arising from these vibrations, with torsional levels that are accessible from the four lowest levels with up to Δm or $\Delta(m_1+m_2) = 6$, for *p*FT and *p*Xyl, respectively. Note that coupling is only expected to occur between levels that have the same nuclear spin symmetry; hence, although a particular vibration may be coupled to other vibrations via interactions between vibtor levels, such interactions will split into two groups for *p*FT and four for *p*Xyl, corresponding to the nuclear spin symmetries of each of the "cold" torsional levels noted earlier, since neither electronic excitation nor the interactions between vibrational or vibtor levels can change the nuclear spin.

Clearly, the more levels that lie close to a ZOB state, the more possibilities there are for coupling, but only a small number of these levels would be expected to couple strongly (i.e. act as "doorway states"), but subsequent couplings and other multistep pathways will be present, leading to widespread interactions of many levels. The numbers noted above and summarized in Table 3, clearly show why there is more interaction between the levels of *p*FT and *p*Xyl compared to *p*ClFB and *p*DFB, and further why the mixing is greater in *p*Xyl than *p*FT. An explicit example of a ZOB state in *p*FT, $2D_{18}$, that is an

overtone of an out-of-plane vibration, being coupled to vibrations of different symmetry via vibtor levels, was discussed in Ref. 39; however, we expect such mechanisms to be widespread.

A summary of the build-up of the vibrations, according to the various criteria outlined above, is provided in Figure 9, where the plots are obtained by summing up the number of levels within 10 cm^{-1} windows (i.e. a DOS plot). A similar plot is presented in Figure 10, where the torsional and vibtor levels have been included for *p*FT and *p*Xyl. It may be seen from Figure 9 that the DOS of totally-symmetric vibrational levels is largely the same across all four molecules. We now consider vibtor levels arising from totally-symmetric vibrations coupled to the "cold" torsional levels, and find that the number of levels that can couple to these increases dramatically for *p*FT and *p*Xyl (Figure 10), while (of course) this changes nothing for *p*DFB and *p*ClFB. When we look at the total numbers of levels of all symmetries, we can see from Figure 10 that there are strong oscillations in the DOS for both *p*DFB and *p*ClFB, while these become less pronounced moving through *p*FT and *p*Xyl. These plots illustrate that the strongest couplings of ZOB states are going to rely on fortuitous coincidences at low wavenumber in *p*DFB and *p*ClFB, explaining why vibrational coupling there consists of the occasional FR. In contrast, even at moderately low wavenumbers, the build-up in levels for *p*FT, and particularly *p*Xyl, illustrates that these coincidences are much more common, indicating widespread mixing of ZOSs and hence the broad unstructured nature of the ZEKE spectra seen when exciting via $S_1 5^1$ in both molecules, and even $S_1 9^1$ in *p*Xyl. The spectra indicate that some of these mixings are strong, and may indicate doorway state behaviour. In Figure 11, we have overlaid the corresponding REMPI spectra on the DOS plots. It may be seen that for D_9 and D_5, the transitions are only coincident with many ZOSs in the cases of *p*FT and *p*Xyl.

Note that these DOS calculations have neglected the methyl-localized vibrations. None of these can couple to D_9, since they are all above 900 cm^{-1}; however, some vibtor levels of these will be in the correct wavenumber region potentially to couple to D_5. Despite this, the number of these falling in a ± 20 cm^{-1} window is not expected to be large, and the trends we see for the D_9 vibration, for which we have noted no contribution is possible, suggests this will be a minor perturbation on the overall picture involving the DOS for D_5.

General comments on IVR

In spectroscopic studies of vibrational interactions (such as IVR) via dispersed fluorescence (DF) or photoelectron spectroscopy (PES), of which ZEKE is an example, one is projecting the S_1 state level(s) onto those of the S_0 state (in DF) or the D_0^+ state (ZEKE). In the absence of vibronic or other interactions, and if the vibrations had identical forms in all three states, and all three states had the

same geometry, then the DF and ZEKE spectra when exciting via a particular S_1 vibrational level would comprise a single $\Delta v = 0$ feature. Of course the geometries of the three states are not expected to be precisely the same, and so we expect to see vibrational activity based on the Franck-Condon principle. If we imagined a *gedanken* experiment where the geometry had changed, but the vibrations all had precisely the same form, then we would see clean activity, including progressions, of vibrations that corresponded to the geometry change between the two states involved; these would only involve vibrations that are totally symmetric in the point group that is common to both states. In reality, deviations from this simple picture can occur from several sources. One would be HT interactions, which (for C_{2v} symmetry) can give rise to new bands from vibrations of different symmetry (such as b_2), but can also affect the intensities of totally-symmetric bands. Another would be Coriolis interactions, which could also give activity in non-totally symmetric bands (but Coriolis effects are not expected to be of importance in jet-cooled studies). Another would be that the changes in geometry will, of course, give rise to changes in the forms of the vibrations, and as such the vibrational activity will alter. We can think of the vibrations in the final states as being made up of linear combinations of those in the intermediate level – i.e. Duschinsky rotation – but this is not vibrational coupling, *per se*. Such effects need to be considered when making conclusions from spectral activity.

In the time domain, discussion often refers to energy flowing through the molecule, populations changing, and vibrational energy becoming redistributed between modes as a function of time. However, in the frequency domain, eigenstates (strictly vibrational eigenstates, as we are ignoring rotations) will have a fixed population and the motion is well-defined. These apparently contradictory pictures are, of course, reconcilable. The issue arises from the fact that time-domain studies use picosecond or even femtosecond pulses, and these have a significant width in wavenumbers, from tens to even hundreds of cm^{-1}. Thus, in these ultrashort laser pulse experiments, a number of eigenstates are usually excited coherently, and indeed it is this that gives rise to the observed time-dependence. If one excites a single uncoupled vibrational state – for example, one that is energetically distant from any other state (i.e. it is a single ZOS) – then no time dependence would be observed whatever the pulse duration. In a similar way, if one excites a single eigenstate that that arises from the interaction of ZOSs, with an ultrashort laser pulse, then of course still no time dependence would be observed.

If we consider the simplest case where two ZOSs interact strongly, one of which is “bright” and the other of which is “dark” then we form two eigenstates, each with a significant character of each of the ZOSs. Further, if these two eigenstates are excited coherently, and with the same probability, then at $t = 0$ the superposition of the two spectra from these will resemble that of the ZOB state (the ZOB

components are in-phase, but the ZOD components are out-of-phase); however, the wavepacket will evolve, and sometime later, the superposition will resemble the ZOD state (the ZOB components are out-of-phase, but the ZOD components are in-phase), and so on – quantum beating. If we interrogate this population in an ultrashort laser experiment, by projecting the population onto the vibrational levels in another state, for example by PES, then we will see the population apparently switching between the ZOB state and the ZOD state, even though the form of the individual eigenstates and their populations are not changing. In more complicated systems, the interactions could give rise to multiple eigenstates contributing to the wavepacket and although at t = 0 it should resemble the ZOB state closely (providing all relevant eigenstates have been excited with equal probabilities), it is possible that rapid dephasing causes any resulting spectrum to become unstructured, even at short times. Still, however, the motions and the populations of the multiple eigenstates will have remained unaltered. In the frequency domain, the idea of IVR is thus really a misnomer, since, as noted above, the populations and motions of the eigenstates are constant, even though these eigenstates could be the result of interactions between a large number of ZOSs. However, the result of such interactions is clearly a wider dispersal of the energy through the molecular degrees of freedom.

The usefulness of the time domain picture can be illustrated by a simple electronic absorption experiment. Clearly, if a ZOS is localized in nature, and poorly coupled to any other level, then its excitation will allow mode-specific excitation to be studied.[14] Alternatively, if a ZOB state is coupled to a number of other ZOSs, and we excite the molecule with an ultrashort laser pulse then, in some circumstances, we will be able to create a wavepacket that resembles the ZOB state long enough that mode-selective excitation can still occur, and reactivity might be controllable. Another useful situation in which to view IVR in the time domain is when a new chemical bond is made in an isolated species, where the initial excitation is localized in the new bond. If this is an uncoupled local mode (or a weakly coupled mode), then the energy cannot be efficiently dissipated, and the bond will break again (the most obvious case of this is that of two atoms colliding to form a diatomic molecule). If, however, the new chemical bond corresponds to a ZOS that is involved in a wide range of coupled vibrational eigenstates, then the bond formation will result in the excitation of this wide range of vibrational eigenstates. Initially, the formed wavepacket will look like the localized ZOS, but the energy is actually shared between many vibrational eigenstates, and the dispersed nature of the ZOSs becomes evident as the vibrational eigenstates dephase.

The present work indicates that the presence of methyl groups in a molecule will make it more difficult to undertake vibrational state-selective experiments, and that the more methyl groups there are, the

more unlikely it will be that selectively is achievable, even if the effective point-group symmetry (i.e. with the assumption of a point mass for the methyl group) of the molecule increases.

4. Concluding remarks

In this work, we have shown that in closely-related species, point group symmetry does not appear to have a large effect on IVR, which is contrary to some other studies.[48,49,50] Two of these studies did not consider jet-cooled molecules,[48,50] and additionally in the ultrafast study[50] a 300 cm^{-1} wide pulse was used in creating the wavepacket, and hence in those experiments other factors are likely playing a role. In addition, two of the studies considered relatively high-lying levels,[49,50] where we would expect the DOS of states to be largely continuous. As a consequence, the IVR behaviour probed in those studies is very different to that here, and illustrates the importance of considering the role of the experimental conditions on conclusions regarding IVR – see discussion in Ref. 30. At low wavenumbers, the erratic build-up of the DOS produces a role for serendipity in whether the wavenumber of a ZOB state coincides with a clump of ZOSs, and indeed whether it can couple to them. The implication of this is, of course, that one can only observe interactions between vibrational levels and, by extension, IVR, in a localized sense. As a consequence, some caution is required in making general conclusions based on a small number of observations.

On the other hand, here and in Ref. 39, we have shown that the presence of methyl groups does play a prominent role, both in the build-up of the DOS, but also in the facilitation of coupling between vibrational levels of different symmetry. Indeed, the effect of the presence of methyl groups appears to outweigh any symmetry effects. We emphasise that these coupling effects are going to be most clearly discernible at low wavenumbers, but will play a role over all wavenumber ranges. We have noted that above-cited early work by Parmenter and coworkers concluded the role of the methyl rotor was significant, and this fits the observation of vibtor states and interactions involving them, seen by our group and that of Lawrance and coworkers (see above citations). The conclusion of von Benten at al.,[40,41] that the presence of a methyl rotor, or $–CF_3$ group, is irrelevant is clearly contradictory to the present and other jet studies. We ascribe this difference in conclusion to the fact that those studies[40,41] were undertaken at significant gas pressures and elevated temperatures, or in solution; and, further, used ultrashort laser pulses so that single eigenstate resolution was not possible (or desirable for those experiments). As a consequence, again we emphasise that the important role played by the experimental conditions in observations on IVR, and making reliable general conclusions is often far from straightforward.

In summary, in the present work, we have examined the ZEKE spectra of four *para*-disubstituted benzene molecules, when exciting via different vibrational levels of the S_1 state over a range of vibrational wavenumbers. This has allowed us to compare the effect of both the point group symmetry and the molecular symmetry group on coupling between vibrational and vibtor levels. In so doing, we have been able to isolate the point group symmetry changes from that of the addition of a methyl group. Moreover, when comparing the behaviour of a molecule with one methyl group (*p*FT) with that of a molecule with two (*p*Xyl), we see *increased* coupling even though we have moved from an asymmetrically-substituted molecule to a symmetrically-substituted one. We have associated this with the increase in the number of torsional levels, which is more than doubled via the in-phase and out-of-phase motions of the two rotors in *p*Xyl. Further, the differing nuclear spin symmetries of the four lowest torsional levels means that these are all populated, even under jet-cooled conditions. In addition, any pure vibrational state gives rise to many vibtor levels, and a number of these will have symmetries that open up routes to coupling between vibrations of different symmetry, via their various vibtor levels.

The appearance of each of the *p*FT and *p*Xyl ZEKE spectra are seen to change significantly even when exciting via levels that are close in wavenumber, implying that these have very different access to the underlying bath of states that is building up with increasing wavenumber, initially erratically, and then continuously (but not uniformly). This restricted access could be the result of weak coupling, and so a more stringent requirement on energetic proximity, and/or it could be the result of symmetry constraints. Some evidence for the serendipity of the possibility of interactions comes from noting that the D_9 vibration is coupled to $2D_{29}$ in *p*ClFB and *p*FT, even though one of the substituents has a significantly different mass, while the same vibration couples to the $2D_{18}$ level in *p*Xyl (where the 29^2 band appears to be exceptionally weak or absent, suggesting little interaction). In the *p*DFB molecule the D_9 level has been hypothesised as being coupled to $2D_{11}$; further, the $2D_{29}$ level is weakly coupled to D_9 in this molecule (where $2D_{29}$ appears to be overlapped, and so apparently not interacting with, the $17^1 19^1$ level). In a similar vein, D_5 does not appear to be coupled to any level in *p*DFB (see above, and Ref. 69), but this vibration is in FR with the $2D_{10}$ level in *p*ClFB;[55,56] while it is clear that there is widespread coupling of D_5 in *p*FT and *p*Xyl, even though there are few pure vibrational levels that are totally symmetric and energetically close.

To gain insight into this, we looked explicitly at the build-up of the vibrational and vibtor levels in the range 0–1400 cm^{-1} in the four molecules and have shown that this gives a clear rationale for the observed behaviour. Further, it indicates the clumpiness of the build-up of vibrational levels for *p*DFB and *p*ClFB, and the dramatic localized increases in the DOS once vibtor levels are included for *p*FT and

*p*Xyl; this build-up is more rapid for *p*Xyl than for *p*FT, owing to larger number of torsional levels that are made of the different combinations of the torsional levels of each methyl group. As we explicitly saw in Ref. 39, but which we expected to be a more general picture, and is confirmed herein, the torsional levels facilitate coupling between vibrational levels of different symmetry, via the creation of many totally-symmetric vibtor levels. Together with other coupling mechanisms, such as HT and Coriolis, there are routes for vibrations of all symmetry classes to interact via their vibtor levels, but still restricted to the same nuclear spin symmetries, and hence a rapid increase in the coupling possibilities.

Overall, the general conclusion from the present work is that the presence of CH_3 groups does indeed increase the propensity for IVR, and appears to override any vibrational symmetry constraints. We anticipate that these ideas will generalize, and cover other low-frequency, wide-amplitude motions, such as NH_2 inversions, alkyl chain bends and so on. In particular, for long, flexible chains attached to phenyl rings, it may be anticipated that there could be interactions with the phenyl-localized out-of-plane modes.

Acknowledgements

We are grateful to the EPSRC for funding (grant EP/L021366/1). The EPSRC and the University of Nottingham are thanked for studentships to W.D.T., D. J. K. and L.E.W. We are grateful to the High Performance Computer resource at the University of Nottingham.

Table 1: Calculated and experimental vibrational wavenumbers for *p*Xyl

D_i	Mulliken (D_{2h})	*p*Xyl			
		S_1		D_0^+	
		Calc [a]	Expt[b]	Calc [c]	Expt[b]
a_1					
D_1	$1(a_g)$	3105		3106	
D_2	$10(b_{1u})$	3088		3093	
D_3	$2(a_g)$	1542		1633	~1634[d]
D_4	$11(b_{1u})$	1437		1450	
D_5	$3(a_g)$	1176	1186[d]	1229	1237[d]
D_6	$12(b_{1u})$	1192	1192	1209	
D_7	$4(a_g)$	1147		1175	1189
D_8	$13(b_{1u})$	959		965	
D_9	$5(a_g)$	784	775[d]	791	805
D_{10}	$14(b_{1u})$	694		693	
D_{11}	$6(a_g)$	402	404	440	439
a_2					
D_{12}	$7(a_u)$	653		994	
D_{13}	$9(b_{1g})$	546	611	782	789
D_{14}	$8(a_u)$	201	217	349	340
b_1					
D_{15}	$15(b_{2g})$	719	669	1005	1007
D_{16}	$28(b_{3u})$	640	595	784	759
D_{17}	$16(b_{2g})$	502		641	639
D_{18}	$29(b_{3u})$	443	400	470	476
D_{19}	$17(b_{2g})$	203	213	232	231
D_{20}	$30(b_{3u})$	104	106	100	102
b_2					
D_{21}	$18(b_{2u})$	3100		3104	
D_{22}	$23(b_{3g})$	3084		3092	
D_{23}	$24(b_{3g})$	1445		1399	
D_{24}	$19(b_{2u})$	1322		1470	
D_{25}	$20(b_{2u})$	1390		1300	
D_{26}	$25(b_{3g})$	1277		1250	
D_{27}	$21(b_{2u})$	920		1133	
D_{28}	$26(b_{3g})$	545	554	553	555
D_{29}	$27(b_{3g})$	367	370	376	378
D_{30}	$22(b_{2u})$	283		289	

[a] TD-DFT B3LYP/aVTZ scaled by 0.97.

[b] Experimental values from Refs. 57 and 58, and present work – see text for details.

[c] UB3LYP/aVTZ scaled by 0.97; $<S^2>$ less than 0.76.

[d] Likely in Fermi resonance – see text.

Table 2

Vib. Symm.		Vibtor Symm.			
D_{2h}	G_{72}	{0,0} – A_1'	{0,1} – G″	{1,1} – E_3'	{1,-1} – E_1'
a_g	a_1'	a_1'	g''	e_3'	e_1'
b_{1g}	a_2'	a_2'	g''	e_4'	e_1'
b_{2g}	a_3''	a_3''	g'	e_3''	e_2''
b_{3g}	a_4''	a_4''	g'	e_4''	e_2''
a_u	a_3'	a_3'	g''	e_3'	e_2'
b_{1u}	a_4'	a_4'	g''	e_4'	e_2'
b_{2u}	a_1''	a_1''	g'	e_3''	e_1''
b_{3u}	a_2''	a_2''	g'	e_4''	e_1''

Table 3: Numbers of vibrational and vibtor levels close to D_9 and D_5

	*p*ClFB	*p*FT	*p*DFB	*p*Xyl
D_9 ± 20 cm^{-1}				
Totally-symmetric vibrational levels	6	6	5	1
Totally-symmetric vibrational and vibtor levels	6	17	5	14
Vibrational levels	30	14	19	18
Total that are accessible from the "cold" torsional levels	6	47	5	169
Total (all symmetries)	30	123	19	595
D_5 ± 20 cm^{-1}				
Totally-symmetric vibrational levels	18	21	7	9
Totally-symmetric vibrational and vibtor levels	18	76	7	81
Vibrational levels	85	91	74	72
Total that are accessible from the "cold" torsional levels	18	221	7	734
Total (all symmetries)	85	610	74	2602

Figure Captions

Figure 1: Structures of the molecules discussed in this work, with their point groups and, where applicable the molecular symmetry group. In designating a point group for *p*FT and *p*Xyl, we are assuming the methyl group is a point mass.

Figure 2: REMPI spectra (0–1400 cm^{-1}) of the four molecules discussed in this work. The assignments are discussed in references given in the text for *p*ClFB, *p*DFB, *p*FT and the 0–600 cm^{-1} region of *p*Xyl. The higher-wavenumber assignments for *p*Xyl are discussed in the present work. The assignments given in red indicate bands which has been used as intermediates in recording presented ZEKE spectra – see text.

Figure 3: ZEKE spectra recorded via the origin of the $S_1 \leftarrow S_0$ transition for the four molecules discussed in the present work. The assignments mainly come from previous work cited in the text – also see text for further discussion. Bands marked with an asterisk for *p*ClFB and *p*DFB are accidental resonances (see Refs. 56 and 60) and not part of the ZEKE spectrum.

Figure 4: ZEKE spectra recorded via the $S_1\ 9^1 \leftarrow S_0$ transition for the four molecules discussed in the present work. The assignments for *p*ClFB, *p*DFB and *p*FT come from previous work cited in the text – also see text for further discussion. The assignments for *p*Xyl are discussed in the text. Bands marked with an asterisk for *p*ClFB and *p*DFB are accidental resonances (see Refs. 56 and 60) and not part of the ZEKE spectrum. The mode diagram for the D_9 vibration from Ref. 51 is shown, and is similar for all four molecules.

Figure 5: ZEKE spectra recorded via the $S_1\ 5^1 \leftarrow S_0$ transition for the four molecules discussed in the present work. The assignments for *p*ClFB, *p*DFB and *p*FT come from previous work cited in the text – also see text for further discussion. The assignments for *p*Xyl are discussed in the text. Bands marked with an asterisk for *p*ClFB and *p*DFB are accidental resonances (see Refs. 56 and 60) and not part of the ZEKE spectrum. Mode diagrams for the D_5 vibration from Ref. 51 are shown, which may be seen to be a symmetric stretch of both C-X bonds (X = F or CH_3) for the symmetrically substituted species, but is a localized C-F stretch for the asymmetrically substituted species – see Ref. 51 for further discussion.

Figure 6: ZEKE spectra for *p*DFB recorded via a series of intermediate states, whose relative wavenumbers in the S_1 state may be seen in Figure 2. Bands marked with an asterisk are accidental resonances (see Ref. 56) and not part of the ZEKE spectrum. Of note is that the spectra are structured with a clean baseline, except for the spectrum via 29^2, which is weak, and the baseline is noisy from the ionization laser intensity variation.

Figure 7: ZEKE spectra for *p*Xyl recorded at different excitation wavenumbers in the region 770–810 cm^{-1} – see section of REMPI spectrum shown – which covers the 9^1 transition. Corresponding letters label the excitation position on the REMPI spectrum and each ZEKE spectrum. A significant rise in the baseline and general deterioration of the structure is evident in some of the spectra – see text for discussion.

Figure 8: ZEKE spectra for *p*Xyl recorded at different excitation wavenumbers in the region 1140–1230 cm^{-1} – see section of REMPI spectrum shown – which covers the 9^1 transition. Corresponding letters label the excitation position on the REMPI spectrum and each ZEKE spectrum. A significant rise in the baseline and general deterioration of the structure is evident in most of the spectra – see text for discussion.

Figure 9: Density of state plots showing the vibrational levels for the four subject molecule, each point in the plot represents the number of vibrations within a 10 cm^{-1} window. It is seen (see text) that the build-up of vibrational levels is relatively low and erratic and fairly consistent between the molecules.

Figure 10: Density of state plots showing the vibrational and vibtor (for *p*FT and *p*Xyl) levels for the four subject molecules – note the different *y*-axis scales for the latter. (Each point in the plot represents the number of vibrations within a 10 cm^{-1} window.) Although the build-up of vibrational levels is relatively low and fairly consistent across the molecules (see Figure 9), the addition of the vibtor levels causes a very significant increase. To low wavenumber the erratic build-up of states is evident, and this is particularly marked for the vibrational levels (see also Figure 9).

Figure 11: Comparison of the density of states build-up with the REMPI spectra for the four subject molecules, for levels accessible from "cold" levels – see test. The sparseness of the DOS for *p*ClFB and *p*DFB makes it clear why just occasional Fermi resonances occur at low wavenumber, while interactions are much more widespread for *p*FT and particularly *p*Xyl.

Figure 1

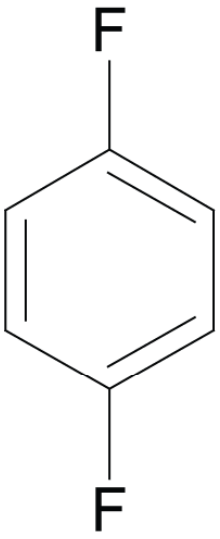

(a) *p*DFB

D_{2h}

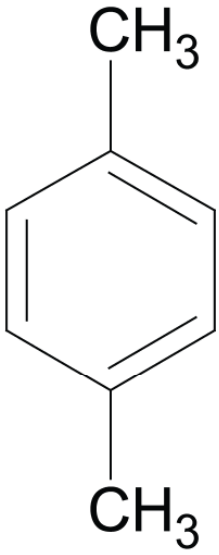

(b) *p*Xyl

D_{2h}/G_{72}

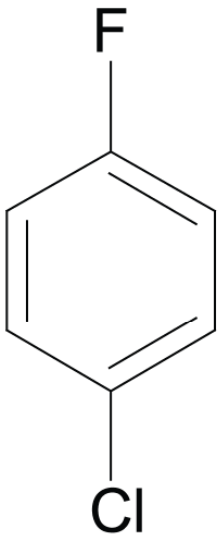

(c) *p*ClFB

C_{2v}

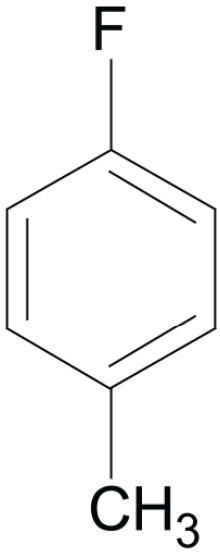

(d) *p*FT

C_{2v}/G_{12}

Figure 2

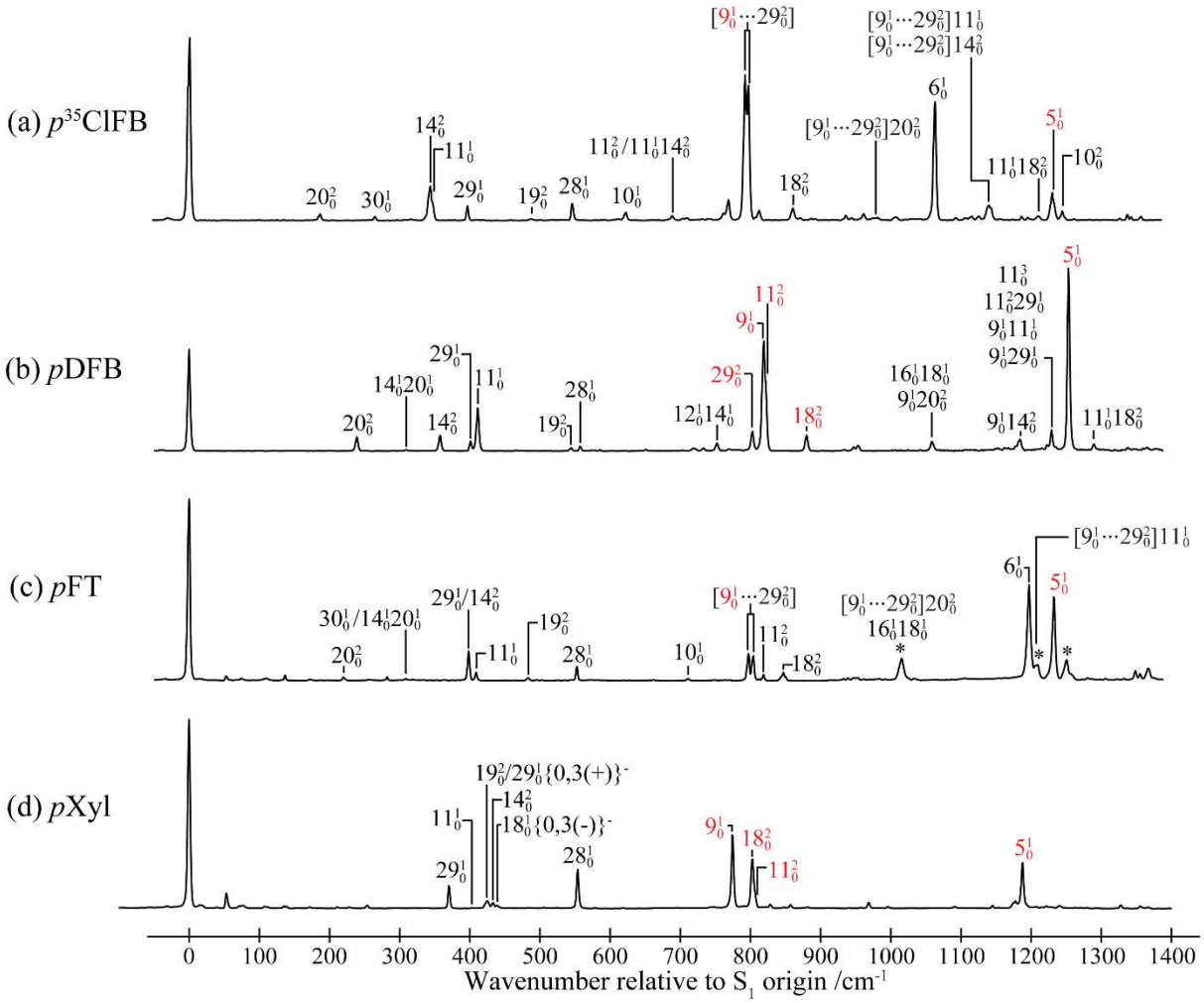
(a) p^{35}ClFB
(b) pDFB
(c) pFT
(d) pXyl
Wavenumber relative to S_1 origin /cm^{-1}
0
100
200
300
400
500
600
700
800
900
1000
1100
1200
1300
1400

Figure 3

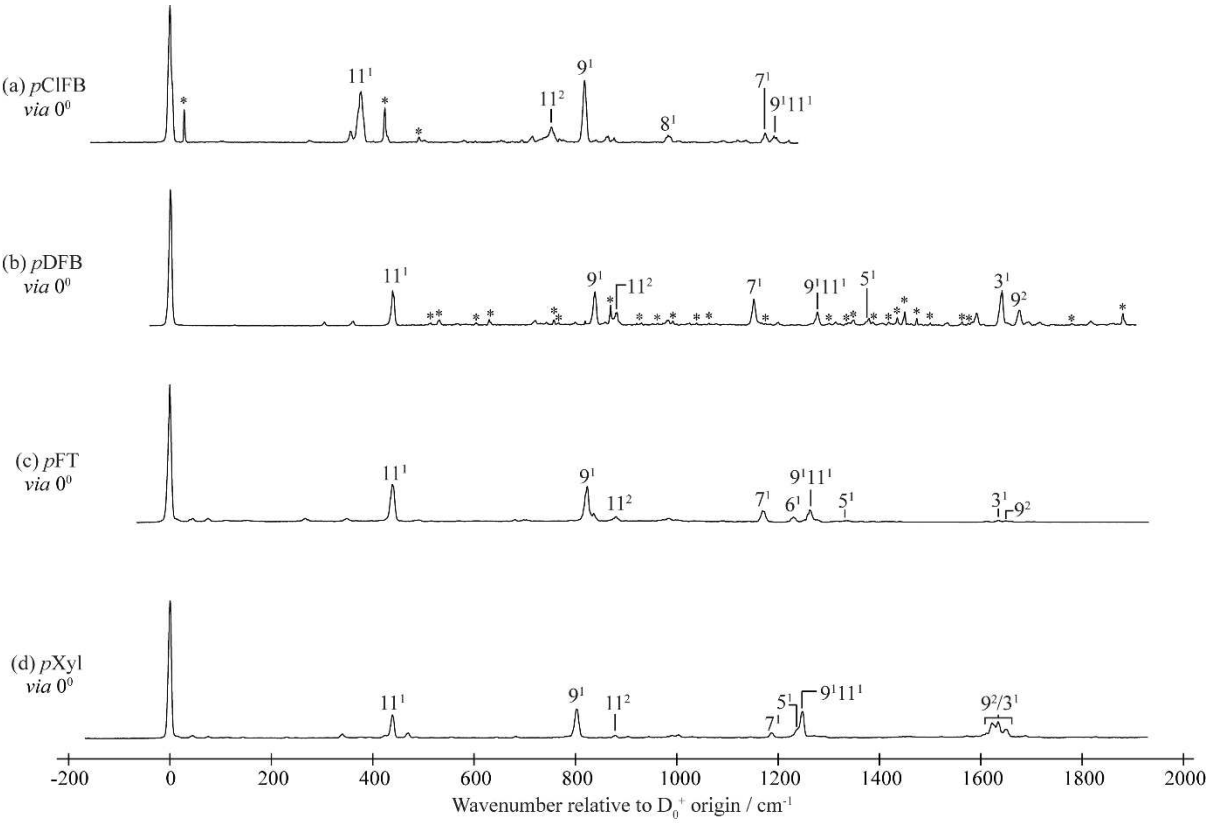
(a) pClFB
via 0⁰
(b) pDFB
via 0⁰
(c) pFT
via 0⁰
(d) pXyl
via 0⁰
11¹
9¹
11²
7¹
8¹
9¹11¹
5¹
3¹
9²
6¹
9²/3¹
-200
0
200
400
600
800
1000
1200
1400
1600
1800
2000
Wavenumber relative to D0+ origin / cm-1

Figure 4

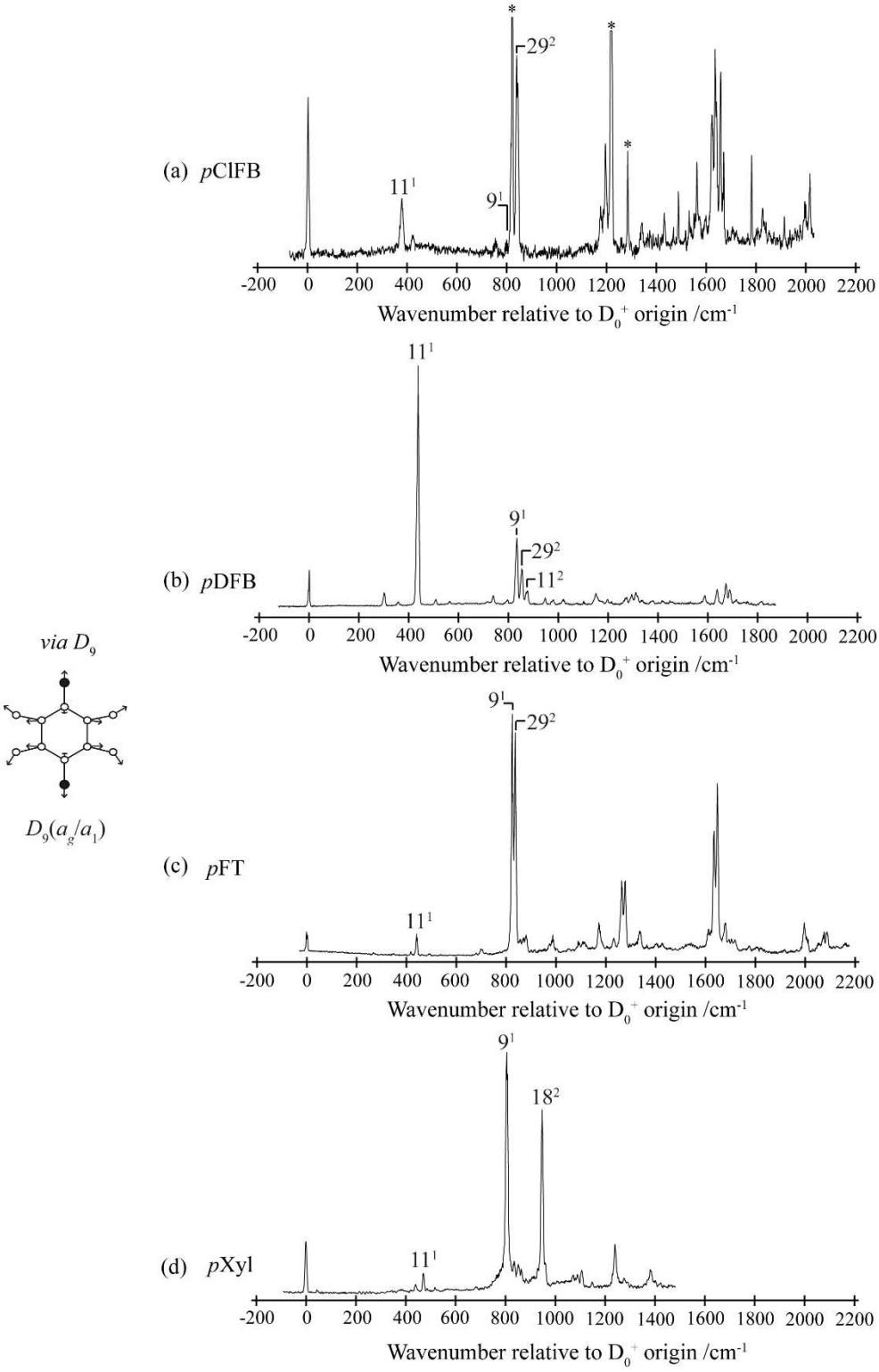
(a) pClFB
(b) pDFB
(c) pFT
(d) pXyl
11¹
9¹
29²
11²
18²
*
-200 0 200 400 600 800 1000 1200 1400 1600 1800 2000 2200
Wavenumber relative to D0+ origin /cm-1
via D9
D9(ag/a1)

Figure 5

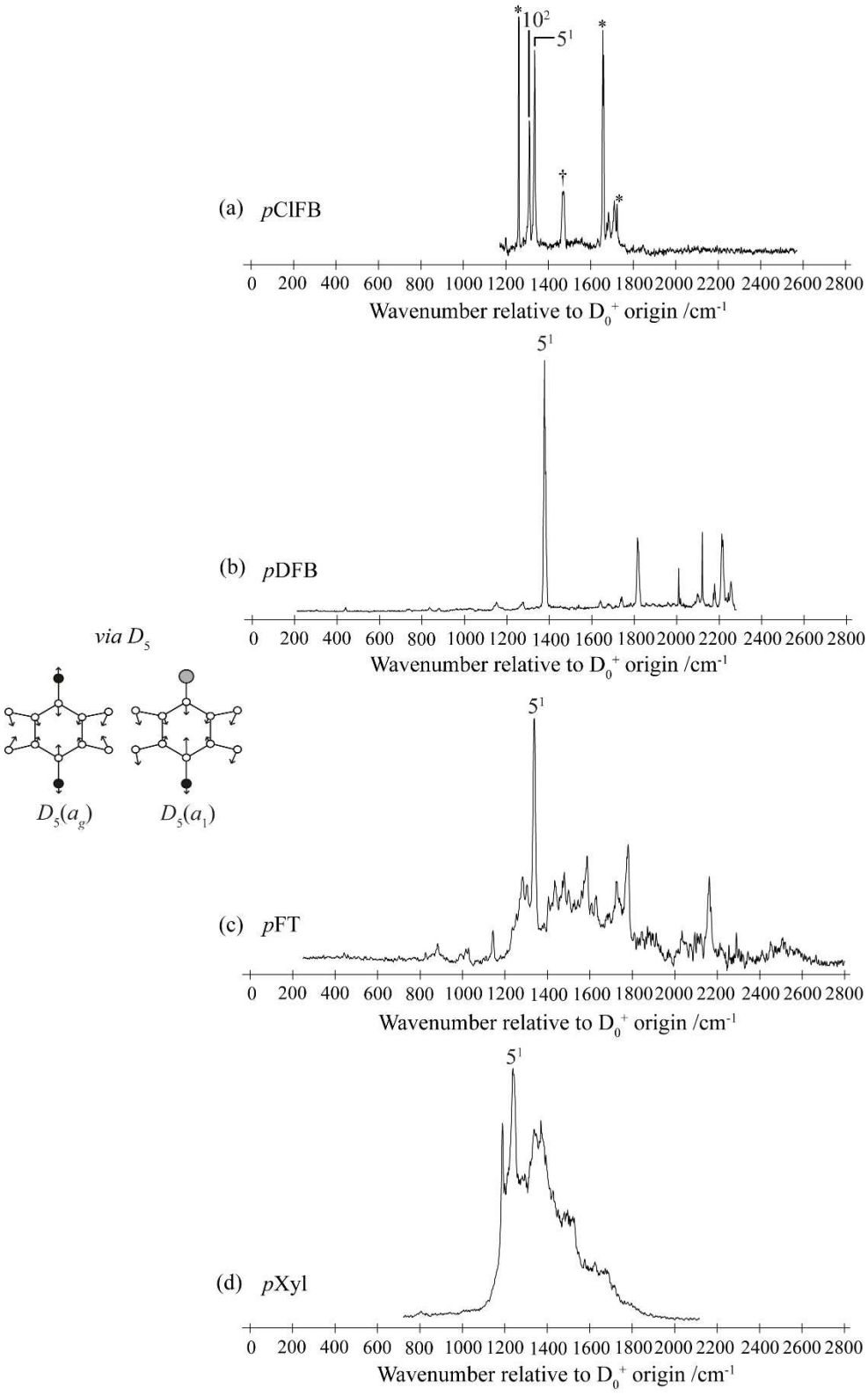
*
10²
5¹
*
†
*
(a) pClFB
0 200 400 600 800 1000 1200 1400 1600 1800 2000 2200 2400 2600 2800
Wavenumber relative to D0+ origin /cm-1
5¹
(b) pDFB
via D5
0 200 400 600 800 1000 1200 1400 1600 1800 2000 2200 2400 2600 2800
Wavenumber relative to D0+ origin /cm-1
D5(ag)
D5(a1)
5¹
(c) pFT
0 200 400 600 800 1000 1200 1400 1600 1800 2000 2200 2400 2600 2800
Wavenumber relative to D0+ origin /cm-1
5¹
(d) pXyl
0 200 400 600 800 1000 1200 1400 1600 1800 2000 2200 2400 2600 2800
Wavenumber relative to D0+ origin /cm-1

Figure 6

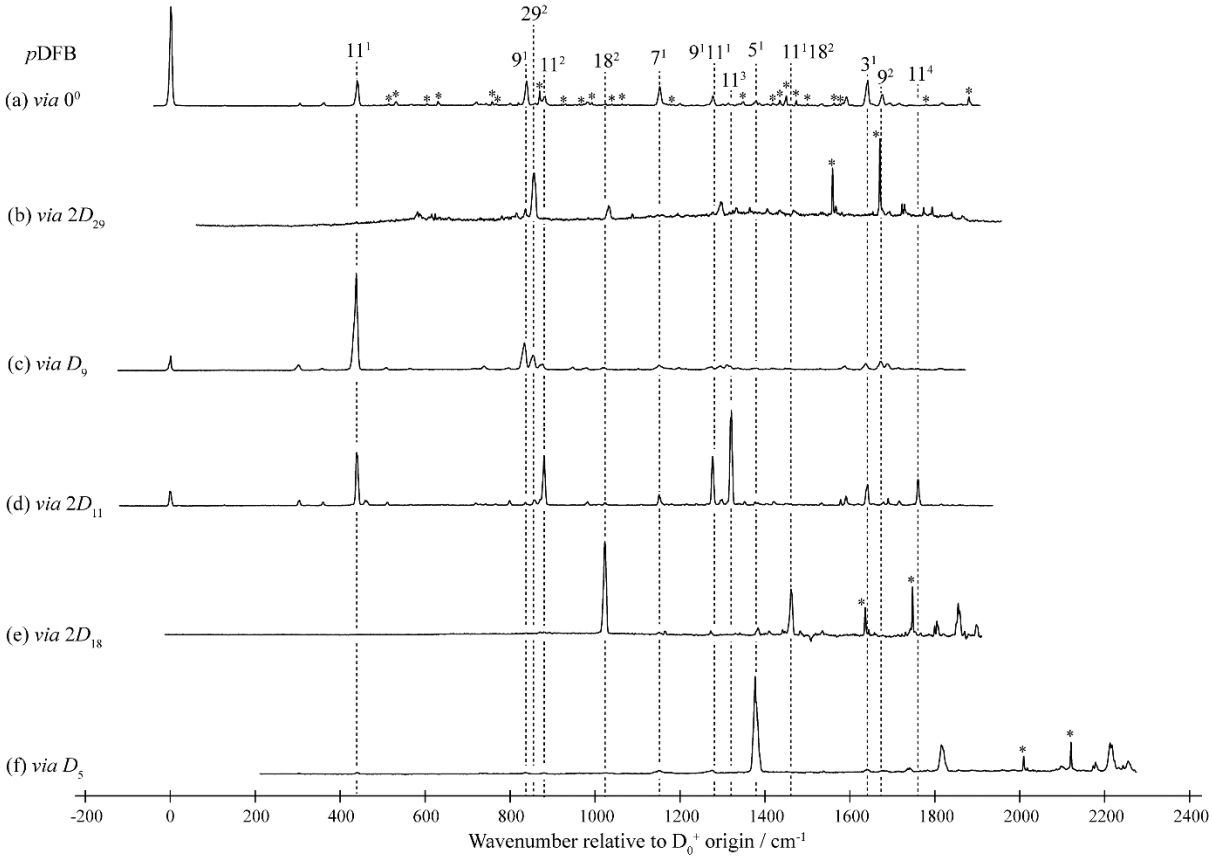
pDFB
(a) via 0⁰
(b) via 2D29
(c) via D9
(d) via 2D11
(e) via 2D18
(f) via D5
29²
11¹
9¹
11²
18²
7¹
9¹11¹
5¹
11³
11¹18²
3¹
9²
11⁴
-200
0
200
400
600
800
1000
1200
1400
1600
1800
2000
2200
2400
Wavenumber relative to D0+ origin / cm-1

Figure 7

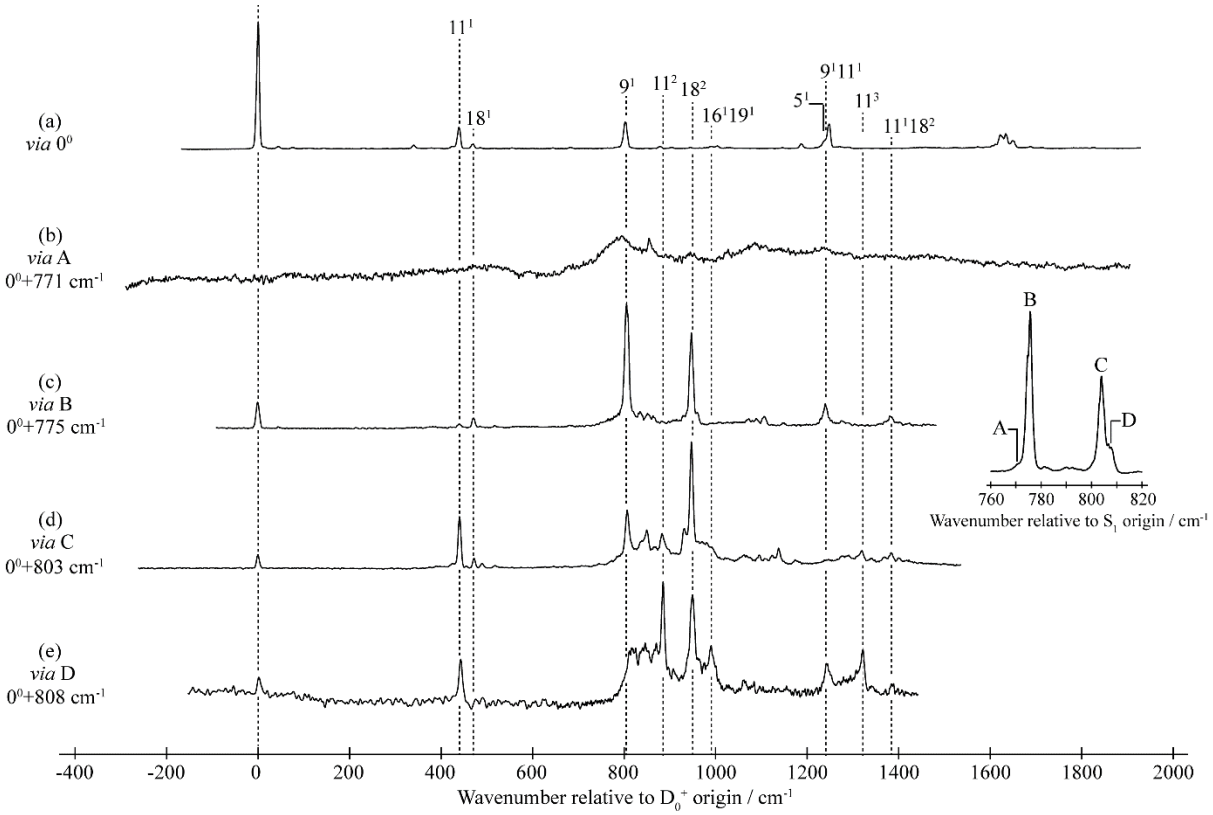
11¹
18¹
9¹
11²
18²
16¹19¹
5¹
9¹11¹
11³
11¹18²
(a)
via 0⁰
(b)
via A
0⁰+771 cm⁻¹
(c)
via B
0⁰+775 cm⁻¹
(d)
via C
0⁰+803 cm⁻¹
(e)
via D
0⁰+808 cm⁻¹
A
B
C
D
760
780
800
820
Wavenumber relative to S1 origin / cm⁻¹
-400
-200
0
200
400
600
800
1000
1200
1400
1600
1800
2000
Wavenumber relative to D0+ origin / cm⁻¹

Figure 8

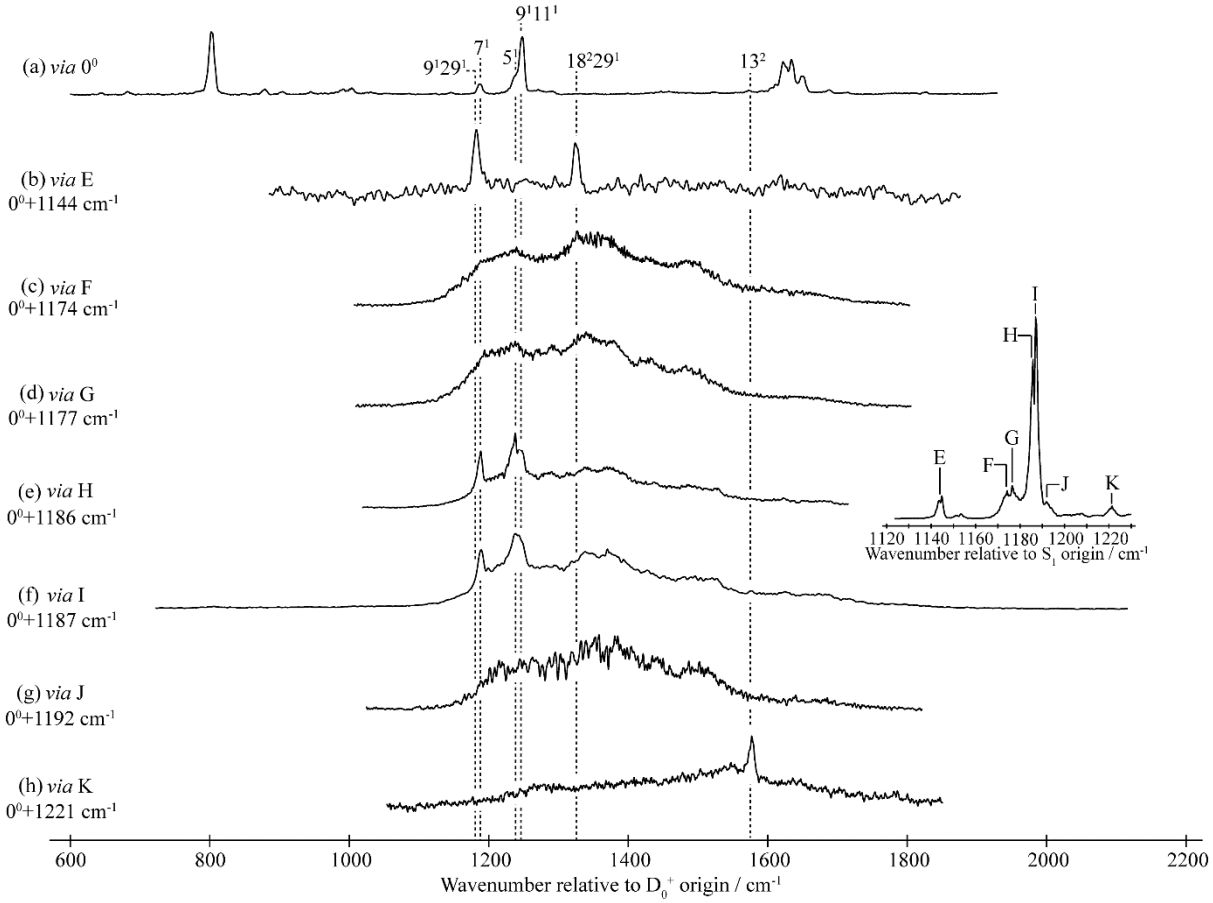
(a) via 0⁰
(b) via E
0⁰+1144 cm⁻¹
(c) via F
0⁰+1174 cm⁻¹
(d) via G
0⁰+1177 cm⁻¹
(e) via H
0⁰+1186 cm⁻¹
(f) via I
0⁰+1187 cm⁻¹
(g) via J
0⁰+1192 cm⁻¹
(h) via K
0⁰+1221 cm⁻¹
9¹11¹
7¹
5¹
9¹29¹
18²29¹
13²
E
F
G
H
I
J
K
1120 1140 1160 1180 1200 1220
Wavenumber relative to S1 origin / cm-1
600 800 1000 1200 1400 1600 1800 2000 2200
Wavenumber relative to D0+ origin / cm-1

Figure 9

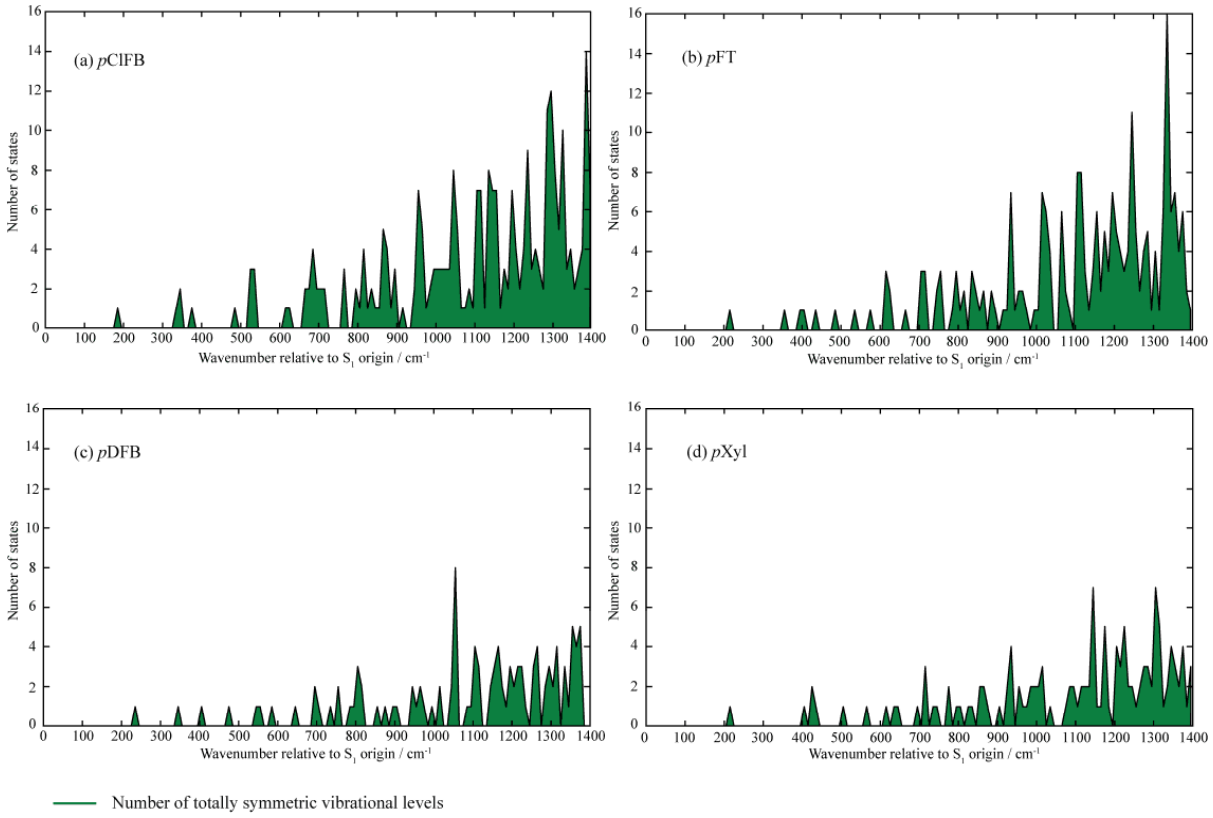
(a) pClFB
(b) pFT
(c) pDFB
(d) pXyl
Number of states
Wavenumber relative to S1 origin / cm-1
Number of totally symmetric vibrational levels

Figure 10

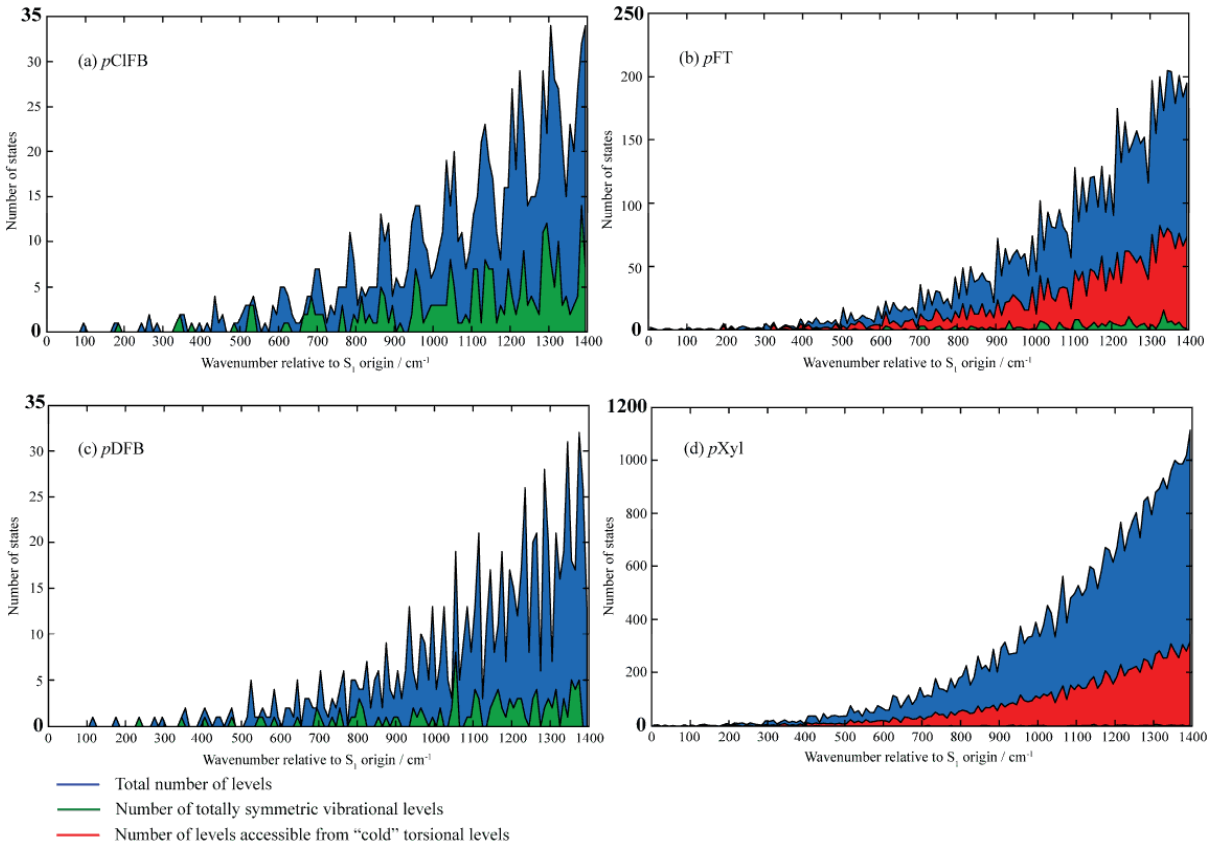
(a) pClFB
(b) pFT
(c) pDFB
(d) pXyl
Number of states
Wavenumber relative to S1 origin / cm-1
Total number of levels
Number of totally symmetric vibrational levels
Number of levels accessible from "cold" torsional levels

Figure 11

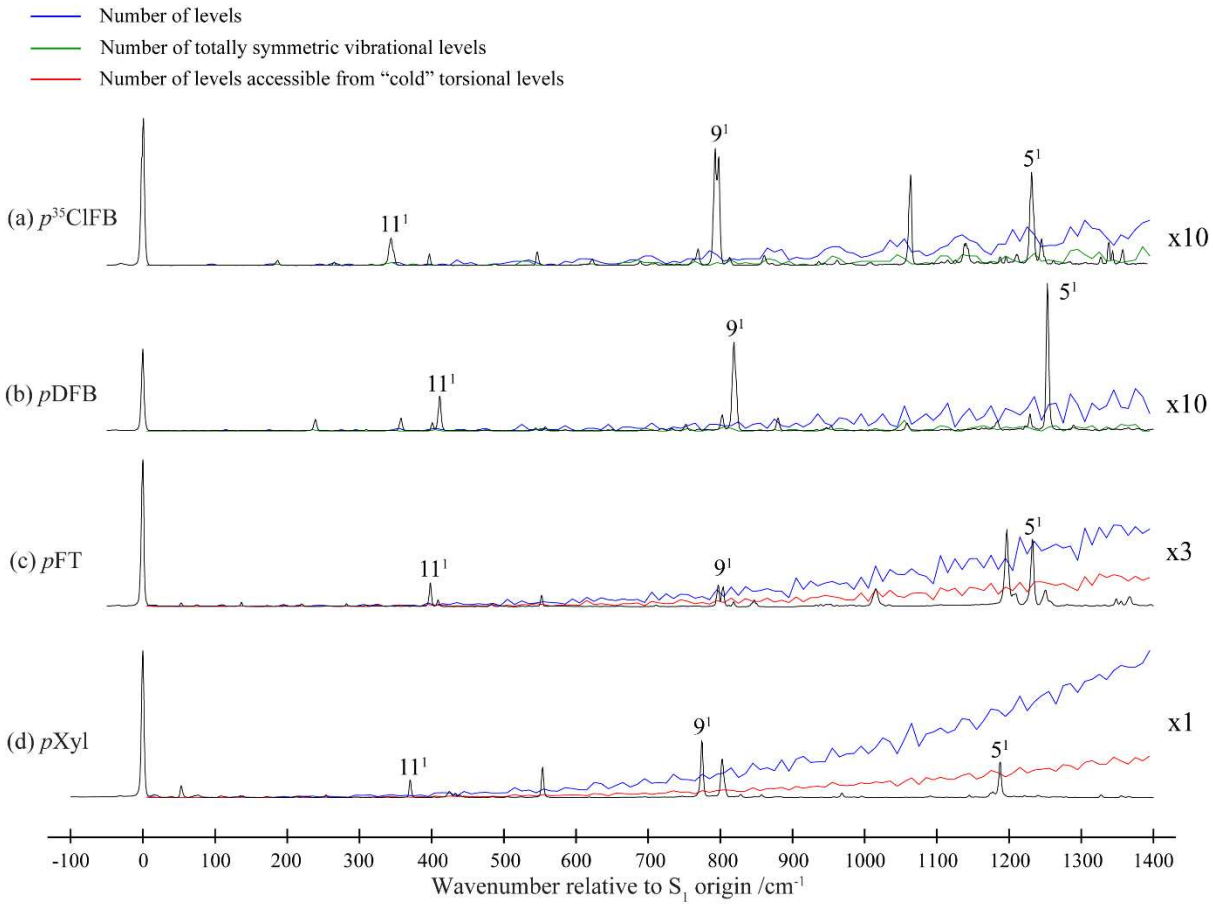
Number of levels
Number of totally symmetric vibrational levels
Number of levels accessible from "cold" torsional levels
(a) p35ClFB
(b) pDFB
(c) pFT
(d) pXyl
11¹
9¹
5¹
x10
x10
x3
x1
-100
0
100
200
300
400
500
600
700
800
900
1000
1100
1200
1300
1400
Wavenumber relative to S1 origin /cm-1

References

[1] G. M. Roberts and V. G. Stavros in *Ultrafast Phenomena in Molecular Sciences*, Ed. R. de Nalda and L. Bañares (Springer, Dordrecht, 2014).

[2] Y. He, C. Wu, and W. Kong, *J. Phys. Chem. A*, 2003, **107**, 5145–5148.

[3] C. Skinnerup Byskov, F. Jensen, T. J. D. Jørgensen, and S. Brøndsted Nielsen, *Phys. Chem. Chem. Phys.*, 2014, **16**, 15831–15838.

[4] P. M. Felker and A. H. Zewail, *J. Chem. Phys*., 1985, **82**, 2961–2974.

[5] P. M. Felker and A. H. Zewail, *J. Chem. Phys.*, 1985, **82**, 2975–2993.

[6] P. M. Felker and A. H. Zewail, *J. Chem. Phys.*, 1985, **82**, 2994–3002.

[7] P. M. Felker, W. R. Lambert and A. H. Zewail, *J. Chem. Phys.*, 1985, **82**, 3003–3010.

[8] D. J. Nesbitt and R. W. Field, *J. Phys. Chem*., 1996, **100**, 12735–12756.

[9] D. Boyall and K. L. Reid, *Chem. Soc. Rev.*, 1997, **26**, 223–232.

[10] K. L. Reid, *Int. Rev. Phys. Chem.*, 2008, **27**, 607–628.

[11] K. K. Lehmann, G. Scoles and B. H. Pate, *Annu. Rev. Phys. Chem.*, 1994, **45**, 241–274.

[12] J. C. Keske and B. H. Pate, *Annu. Rev. Phys. Chem.*, 2000, **51**, 323–353.

[13] E. R. Gonzaga, *Am. J. Clin. Dermat.*, 2009, **10** Suppl. 1, 19–24.

[14] D. R. Killalea and A. L. Utz, *Phys. Chem. Chem. Phys*., 2013, **15**, 20545.

[15] See, for example: F. Di Giacomo, *J. Chem. Ed*., 2015, **92**, 476.

[16] S. Yan, Y.-T. Wu, B. Zhang, X.-F. Yue and K. Liu, *Science*, 2007, **316**, 1723.

[17] J. C. Polanyi, *Acc. Chem. R*es., 1972, **5**, 161.

[18] N. D. N. Rodrigues, M. Staniforth and V. G. Stavros, *Proc. Roy. Soc. A*, 2016, **472**, 20160677.

[19] L. A. Baker, B. Marchetti, T. N. V. Karsili, V. G. Stavros and M. N. R. Ashfold, *Chem. Soc. Rev.*, 2017, **46**, 3770–3791.

[20] A. D. G. Nunn, R. S. Minns, R. Spesyvtsev, M. J. Bearpark, M. A. Robb and H. H Fielding, *Phys. Chem. Chem. Phys.*, 2010, **12**, 15751–15759.

[21] G. A. King, T. A. A. Oliver, R. N. Dixon and M. N. R. Ashfold, *Phys. Chem. Chem. Phys.* **14**, 3338 (2012).

[22] J. R. Gascooke and W. D. Lawrance, *J. Chem. Phys*., 2013, **138**, 134302.

[23] J. A. Davies, A. M. Green, and K. L. Reid, *Phys. Chem. Chem. Phys.*, 2010, **12**, 9872–9883.

[24] J. A. Davies, A. M. Green, A. M Gardner, C. M. Withers, T. G. Wright, and K. L. Reid, *Phys. Chem. Chem. Phys.*, 2014, **16**, 430–443.

[25] J. R. Gascooke, E. A. Virgo, and W. D. Lawrance, *J. Chem. Phys.*, 2015, **143**, 044313.

[26] J. A. Davies and K. L. Reid, *Phys. Rev. Lett.*, 2012, **109**, 193004.

[27] E. A. Virgo, J. R. Gascooke and W. D. Lawrance, *J. Chem. Phys.*, 2014, **140**, 154310.

[28] D. A. Dolson, C. S. Parmenter and B. M. Stone, *Chem. Phys. Lett.* **81**, 360 (1981).

[29] A. A. Makarov, A. L. Malinovsky and E. A. Ryabov, *Physics–Uspekhi*, 2012, **55**, 977.

[30] C. J Hammond, V. L. Ayles, D. Bergeron, K. L. Reid and T. G. Wright, *J. Chem. Phys.*, 2006, **125**, 124308.

[31] C. S. Parmenter and B. M. Stone, *J. Chem. Phys.*, 1986, **84**, 4710.

[32] Q. Ju, C. S. Parmenter, T. A. Stone and Z.-Q. Zhao, *Isr. J. Chem.*, 1997, **37**, 379.

[33] J. S. Baskin, T. S. Rose, and A. H. Zewail, *J. Chem. Phys.*, 1988, **88**, 1458.

[34] D. B. Moss and C, S, Parmenter, *J. Chem. Phys.*, 1993, **98**, 6897.

[35] D. B. Moss, C. S. Parmenter and G. E. Ewing, *J. Chem. Phys.*, 1987, **86**, 51.

[36] Z.-Q. Zhao, C. S. Parmenter, D. B. Moss, A. J. Bradley, A. E. W. Knight, and K. G. Owens, *J. Chem. Phys.*, 1992, **96**, 6362.

[37] Z.-Q. Zhao, PhD Thesis, Indiana University (1992).

[38] Z.-Q. Zhao and C. S. Parmenter, *Mode Selective Chemistry* (Kluwer, 1991) Eds. J. Jortner, R. D. Levine, and B. Pullman. *Jerusalem Symp. Quant. Chem. Biochem*., 1991, **24**, 127.

[39] A. M. Gardner, W. D. Tuttle, L. E. Whalley, and T. G. Wright, *Chem. Sci.*, 2018, **9**, 2270.

[40] R. S. von Benten, Y. Liu and B. Abel, *J. Phys. Chem.* A, 2010, **114**, 11522.

[41] J. Aßmann, M. Kling and B. Abel, *Angew. Chem. Int. Ed. Engl*., 2003, **42**, 2226.

[42] D. P. Mukhopadhyay, S. Biswas and T. Chakraborty, *J. Phys. Chem. A,* 2016, **120**, 9159.

[43] D. P. Mukhopadhyay, S. Biswas and T. Chakraborty, *Chem. Phys. Lett.*, 2017, **674**, 71.

[44] J. A. Davies, L. E. Whalley and K. L. Reid, *Phys. Chem. Chem. Phys.*, 2017, **19**, 5051.

[45] G. A. Bethardy, X. Wang and D. S. Perry, *Can. J. Chem*., 1994, **72**, 652.

[46] D. S. Perry, G. A. Bethardy and X. Wang, *Ber. Bunsenges. Phys. Chem.*, 1995, **99**, 530.

[47] C. C. Martens and W. P. Reinhardt, *J. Chem. Phys*., 1990, **93**, 5621.

[48] L. W. Peng, B. W. Keelan, D. H. Semmes and A. H. Zewail, *J. Phys. Chem.*, 1988, **92**, 554.

[49] M. Hippler, R. Pfab, and M. Quack*, J. Phys. Chem. A*, 2003, **107**, 10743.

[50] R. S. von Benten, Y. Liu, and B. Abel, *J. Chem. Phys.*, 2010, **133**, 134306.

[51] A. Andrejeva, A. M. Gardner, W. D. Tuttle and T. G. Wright, *J. Molec. Spectrosc.*, 2016, **321**, 28–49.

[52] V. L. Ayles, C. J. Hammond, D. E. Bergeron, O. J. Richards and T. G. Wright, *J. Chem. Phys.*, 2007, **126**, 244304.

[53] A. M. Gardner, W. D. Tuttle, L. Whalley, A. Claydon, J. H. Carter and T. G. Wright, *J. Chem. Phys.,* 2016, **145**, 124307.

[54] W. D. Tuttle, A. M. Gardner, L. E. Whalley, and T. G. Wright, *J. Chem. Phys.*, 2017, **146**, 244310.

[55] W. D. Tuttle, A. M. Gardner and T. G. Wright, *Chem. Phys. Lett.*, 2017, **684**, 339.

[56] D. J. Kemp, L. E. Whalley, W. D. Tuttle, A. M. Gardner, B. T. Speake and T. G. Wright, *Phys. Chem. Chem. Phys.*, 2018, DOI: 10.1039/C8CP01274A

[57] A. M. Gardner, W. D. Tuttle, P. Groner, and T. G. Wright, *J. Chem. Phys.*, 2017, **146**, 124308.

[58] W. D. Tuttle, A. M. Gardner, K. B. O'Regan, W. Malewicz, and T. G. Wright, *J. Chem. Phys.*, 2017, **146**, 124309.

[59] D. Rieger, G. Reiser, K. Müller-Dethlefs, and E. W. Schlag, *J. Phys. Chem.*, 1992, **96**, 12.

[60] G. Reiser, D. Rieger, T. G. Wright, K. Müller-Dethlefs and E. W. Schlag, *J. Phys. Chem.*, 1993, **97**, 4335.

[61] S. D. Gamblin, S. E. Daire, J. Lozeille, and T. G. Wright, *Chem. Phys. Lett.*, 2000, **325**, 232.

[62] X. Zhang, J. M. Smith, and J. L. Knee, *J. Chem. Phys.*, 1992, **97**, 2843.

[63] P. M. Felker and A. H. Zewail, *Adv. Chem. Phys.*, 1988, **70**, 265.

[64] D. R. Demmer, J. W. Hager, G. W. Leach and S. C. Wallace, *Chem. Phys. Lett.*, 1987, **136**, 329.

[65] W. D. Lawrance and J. R. Gascooke, Pervasive interactions between methyl torsion and low frequency vibrations in S_0 and S_1 *p*-fluorotoluene. *J. Chem. Phys. (submitted).*

[66] E. Sekreta, K. S. Viswanathan, and J. P. Reilly, *J. Chem. Phys.*, 1989, **90**, 5349.

[67] C. H. Kwon, H. L. Kim and M. S. Kim, *J. Chem. Phys.*, 2003, **118**, 6327.

[68] R. A. Coveleskie and C. S. Parmenter, *J. Molec. Spectrosc.*, 1981, **86**, 86.

[69] A. E. W. Knight and S. H. Kable, *J. Chem. Phys.*, 1988, **89**, 7139.

[70] B. T. Darling and D. M. Denison, *Phys. Rev.*, 1940, **57**, 128.